

1 **A Factorial Bayesian Copula Framework for Partitioning Uncertainties in**
2 **Multivariate Risk Inference**

3
4 Y. Fan^{1*}, K. Huang², G.H. Huang^{3,4*}, Y.P., Li⁴

5
6 ¹Department of Civil and Environmental Engineering, Brunel University, London, Uxbridge,
7 Middlesex, UB8 3PH, United Kingdom

8 ² Faculty of Engineering and Applied Sciences, University of Regina, Regina, SK, Canada

9 ³ Institute for Energy, Environment and Sustainable Communities, University of Regina, Regina,
10 Saskatchewan, Canada S4S 0A2

11 ⁴ School of Environment, Beijing Normal University, Beijing, China, 100875

12
13 *Correspondence: Dr. Y. Fan

14 Department of Civil and Environmental Engineering,
15 Brunel University London,
16 Uxbridge, Middlesex, UB8 3PH, United Kingdom
17 Tel: +44 1895265717
18 Email: yurui.fan@brunel.ac.uk

19
20 Dr. G. H. Huang
21 Institute for Energy, Environment and Sustainable Communities,
22 University of Regina, Regina, Saskatchewan, Canada S4S 0A2,
23 Tel: +1 306 585-4095;
24 Fax: +1 306 585-4855;
25 E-mail: huang@iseis.org

1
2
3
4
5
6
7
8
9
10
11
12
13
14
15
16
17
18
19
20
21
22
23
24
25
26
27
28
29
30
31
32
33
34
35
36
37
38
39
40
41
42
43
44
45
46
47
48
49
50
51
52
53
54
55
56
57
58
59
60
61
62
63
64
65

28 **Abstract:**

29

30 In this study, a factorial Bayesian copula (FBC) method is proposed to quantify
31 parameter uncertainty in copula-based models and then reveal their contributions to
32 the multivariate hydrologic risk inference. In detail, Bayesian inference and factorial
33 analysis are integrated into copula-based multivariate risk models to (1) quantify
34 parameter uncertainties, (ii) reveal their individual and interactive effects, and (iii)
35 identify their detailed contributions on uncertain risk inference. Streamflow
36 observations at Xiangxi and Wei River basins of China are used to illustrate the
37 applicability of FBC. The results indicate that imprecise parameters in marginal
38 distributions and the dependence structure would lead to extensive uncertainties in
39 predictive joint return periods and failure probabilities. Also, individual and
40 interactive effects of parameters are well revealed through multilevel factorial
41 analysis, and the detailed contributions of one parameter to different failure
42 probabilities under different service time scenarios are identified.

43

44 **Keywords:** Flood risk; Copula; Markov chain Monte Carlo; Factorial Analysis;
45 Uncertainty

46

47

1
2
3
4
5
6
7
8
9
10
11
12
13
14
15
16
17
18
19
20
21
22
23
24
25
26
27
28
29
30
31
32
33
34
35
36
37
38
39
40
41
42
43
44
45
46
47
48
49
50
51
52
53
54
55
56
57
58
59
60
61
62
63
64
65

1. Introduction

Flooding, as one of the most frequently occurred natural hazards, has taken a devastating societal and economic toll over the world, leading to a large number of fatalities and property losses. (Kidson and Richards, 2005; Karmakar and Simonovic, 2009; Fan et al., 2015a, b; Huang et al., 2019; Lindenschmidt and Rokaya, 2019; Wu et al., 2019). Assessment and management of flood risks concerns many government agencies, academic institutions as well as individual stakeholders. However, hydrometeorological processes are recognized as multivariate phenomena characterized by dependent multi-attribute properties (Sarhadi et al., 2016). Accordingly, a typical flood event generally presents multiple features such as peak discharge, hydrograph volume and duration. Univariate risk analyses, mainly focusing on flood peaks, cannot procure a full description of the probability of occurrence of the hydrological event (Chebana and Ouarda, 2011; Requena et al., 2013). Consequently, multivariate approaches are recommended by many studies since they can involve a number of non-independent variables for the characterization of a flood (The European Parliament and The Council, 2007; Li et al., 2015; Fan et al., 2016a, b; Salvadori et al., 2016).

The applications of multivariate hydrologic risk analysis are growing dramatically since the introduction of copulas in hydrology and geosciences (Serinaldi, 2013). De Michele and Salvador (2003) initially introduced the concept of copulas into hydrological simulation to describe the dependence between storm duration and average rainfall intensity. After that, a great number of research works have been proposed for multivariate hydrologic simulation through copula functions, such as multivariate flood frequency analysis (Zhang and Singh 2006; Sraj et al., 2014); drought assessments (Song and Singh 2010; Kao and Govindaraju 2010); storm or rainfall dependence analysis (Zhang and Singh 2007; Vandenberghe et al. 2010);

1 77 streamflow simulation (Lee and Salas 2011; Kong et al., 2015; Fan et al., 2017).
2 78 Copulas can model nonlinear dependence between two or more depended variables
3
4 79 with different marginal distributions and relax assumptions of same family of
5
6 80 distributions and linear relationship in traditional multivariate techniques (Zhang and
7
8 81 Singh, 2006; Genest and Favre, 2007; Karmakar and Simonovic, 2009; Sraj et al.,
9
10 82 2014; Huang et al., 2017).

11
12 83
13
14 84 One major issue in hydrologic risk analysis is the presence of uncertainties, resulting
15
16 85 from model selection and parameter estimation. There are two primary sources of
17
18 86 uncertainty: (1) natural uncertainty stemming from variability of the underlying
19
20 87 stochastic process, and (2) epistemic uncertainty coming from incomplete knowledge
21
22 88 about the system under study (Merz and Thielen, 2005). In particular, the limited
23
24 89 sample size of hydrological data implies large uncertainty on the extreme quantiles
25
26 90 (Serinaldi, 2013). Uncertainty assessment is a prominent aspect in univariate
27
28 91 frequency analysis and it is also quite crucial in multivariate framework. Several
29
30 92 research works have been proposed for evaluating uncertainties in copula-based
31
32 93 multivariate risk framework (Serinaldi, 2013; Dung et al. 2015; Zhang et al., 2015).
33
34 94 For instance, Serinaldi (2013) proposed a Monte Carlo-based approach to generate
35
36 95 confidence intervals around p-level curves to account for uncertainties in joint
37
38 96 quantile. These research works demonstrate that significant uncertainties exist in
39
40 97 copula-based hydrologic risk assessment. However, one major issue to be addressed is
41
42 98 to characterize the major sources that lead to uncertainties in multivariate risk
43
44 99 predictions. In a multivariate framework, uncertainties in both marginal distributions
45
46 100 and dependence structures may lead to varied risk predictions. However, few research
47
48 101 studies have been reported to answer which source contributes most to the uncertainty
49
50 102 in the resulting risk predictions.

51
52 103
53
54 104 Consequently, this study aims to propose a factorial Bayesian copula (FBC)
55
56 105 framework to quantify uncertainties in multivariate risk analysis and further partition
57
58 106 sources in the uncertain risk inference. This approach integrates copula model,
59
60
61
62
63
64
65

107 Bayesian parameter estimation and multilevel factorial analysis into a framework. In
108 detail, the multivariate risk inference models in terms of joint return periods and
109 failure probabilities (FPs) are established based on copulas. Parameter uncertainties in
110 marginal distributions and dependence structure are quantified by a Bayesian based
111 Markov Chain Monte Carlo (MCMC) algorithm. Finally, individual and interactive
112 effects of parameter uncertainties are revealed by multilevel factorial analysis. Flood
113 data at three hydrological gauge stations in China are used to illustrate the
114 applicability of the proposed method.

116 **2. Methodology**

117 The proposed FBC approach mainly consists of three components, including: (i)
118 establishment of copula-based multivariate risk assessment model, (ii) quantification
119 of parameter uncertainties and (iii) characterization of contributions of parameters to
120 uncertainties in risk inference. Figure 1 illustrates the detailed procedures for FBC.

122 **2.1. Copula-based Multivariate Risk Assessment**

123
124 In the hydrology context, many hazard events may present with multivariate
125 characteristics. For instance, floods are generally characterized by its peak and
126 volume values, while droughts have multi-attribute of severity and duration. Also,
127 these multi-attributes in one hydrological hazard are usually correlated. To reveal the
128 dependence among the multiple features in one hazard and characterize the associated
129 risk in a multivariate framework, the copulas, initially introduced into hydrology by
130 [Favre et al. \(2004\)](#), have been widely used. The applicability of copulas is mainly
131 attributed to their flexibility in modelling dependence among correlated variables with
132 different marginal distributions. Also, a variety of dependence structures, such as
133 asymmetry, nonlinear and tail dependence, are able to be captured by copulas ([Sarhadi
134 et al., 2016](#)).

136 Consider one hydrological hazard has d correlated attributes (e.g. peak, volume and
 137 duration for a flood) with each one denoted by a random variable X_i ($i = 1, 2, \dots, d$). If
 138 the corresponding probability distributions are denoted as $F_1(x_1|\gamma_1)$, $F_2(x_2|\gamma_2)$, ...,
 139 $F_d(x_d|\gamma_d)$, where $\gamma_1, \gamma_2, \dots, \gamma_d$ are parameters in probability distributions, the joint
 140 probability distribution of X_1, X_2, \dots, X_d can be expressed as (Nelsen, 2006):

$$141 \quad F(x_1, \dots, x_d | \gamma_1, \dots, \gamma_d, \theta) = C(F_1(x_1 | \gamma_1), \dots, F_d(x_d | \gamma_d) | \theta) \quad (1)$$

142 where $C(\cdot)$ is a copula function; θ is the parameter in the copula function describing
 143 dependence among those correlated variables. More details on theoretical background
 144 and properties of various copulas can be found in Nelsen (2006).

145
 146 Through the probability distribution in Equation (1), some features of the hazardous
 147 event can be revealed. Firstly, the concept of return period (RP) is of great importance
 148 in water resources and civil engineering for (i) designing and sizing hydraulic
 149 structures, (ii) identifying dangerous events, (iii) making rational making, and (iv)
 150 assessing related risk (Salvadori et al., 2013). In a multivariate context, the RP of one
 151 specific hazardous event should consider the interaction among different attributes in
 152 the hazardous scenarios, leading to multivariate RP. A number of literatures have been
 153 proposed to characterize multivariate RP in hydrologic issues (Salvadori et al., 2007;
 154 2011; 2013, 2016; Fan et al., 2016a, b). In general, consider one kind of hydrological
 155 extreme (denoted as \mathbf{X}) with d attributes (i.e. $\mathbf{X} = (X_1, X_2, \dots, X_d)$), three categories of
 156 multivariate RP are widely used for hydrologic risk assessment.

157
 158 (i) "OR" case: $T^{OR} = \{(x_1, x_2, \dots, x_d) \in R^d : x_1 > x_1^* \vee x_2 > x_2^* \vee \dots \vee x_d > x_d^*\}$, which
 159 indicates at least one element surpass the predefined threshold. Based on the copula
 160 function, the multivariate RP in "OR" case can be expressed as:

$$161 \quad T^{OR} = \frac{\mu}{1 - C(F_1(x_1 | \gamma_1), \dots, F_d(x_d | \gamma_d) | \theta)} \quad (2)$$

162 where μ denotes the average time between two adjacent events under consideration.

163

164 (ii) “AND” case: $T^{AND} = \{(x_1, x_2, \dots, x_d) \in R^d : x_1 > x_1^* \wedge x_2 > x_2^* \wedge \dots \wedge x_d > x_d^*\}$ which
 165 indicates at all elements in the extreme events should exceed the corresponding
 166 thresholds. Based on the copula function, the multivariate RP in “AND” case can be
 167 expressed as:

$$168 \quad T^{AND} = \frac{\mu}{\hat{C}(\bar{F}_1(x_1 | \gamma_1), \bar{F}_2(x_2 | \gamma_2), \dots, \bar{F}_d(x_d | \gamma_d) | \theta)} \quad (3)$$

169 where \hat{C} is multivariate survival function of the X_i 's proposed by [Salvadori et al.](#)
 170 (2013; 2016), and $\bar{F}_i(x_i | \gamma_i) = P(X > x_i) = 1 - F_i(x_i | \gamma_i)$. Following [Salvadori et al.](#)
 171 (2013; 2016), and the Inclusion-Exclusion principle proposed by [Joe \(2014\)](#), the
 172 multivariate survival function \hat{C} can be obtained by:

$$173 \quad \hat{C}(\mathbf{u}) = \bar{C}(1 - \mathbf{u}) \quad (4)$$

174 and

$$175 \quad \bar{C}(\mathbf{u}) = 1 - \sum_{i=1}^d u_i + \sum_{S \in \mathcal{P}} (-1)^{\#(S)} C_S(u_i : i \in S) \quad (5)$$

176
 177 (iii) “Kendall” case: The Kendall RP is to characterize the hydrologic disasters
 178 exceeding a critical layer defined by ([Salvadori et al., 2011](#)): $L_t^F = \{\mathbf{x} \in R^d : F(\mathbf{x}) = t\}$.
 179 The Kendall RP can be expressed as ([Salvadori et al., 2011](#)):

$$180 \quad T^{Kendall} = \frac{\mu}{1 - K_C(t)} \quad (6)$$

181 where K_C is the Kendall's distribution function associated with C , which can be
 182 expressed as:

$$183 \quad K_C(t) = P(C(F_1(x_1 | \gamma_1), \dots, F_d(x_d | \gamma_d) | \theta) \leq t) \quad (7)$$

184
 185 In addition to the multivariate RP, [Serinaldi \(2015\)](#) recently proposed the notion of
 186 failure probability (FP) to provide more coherent, general and well devised tools for
 187 risk assessment and communication. In general, the failure probability p_M to indicate

188 the occurrence of a critical event for at least one time in M years of design life can be
 189 defined as (Serinaldi, 2015):

$$190 \quad p_M = 1 - \prod_{j=1}^M (1 - p_j) = 1 - (F(x_d))^M \quad (8)$$

191 Similar to the multivariate RP concept, the failure probability (FP) in a multivariate
 192 context can also be characterized in “OR”, “AND”, and “Kendall” scenarios
 193 expressed by the following equations. For a given critical threshold

194 $\mathbf{x}^* = \{x_1^*, x_2^*, \dots, x_d^*\}$, the failure probabilities violating this critical value can be

195 expressed as (Salvadori et al., 2016):

$$196 \quad p_T^{OR} = 1 - (C(F_1(x_1^* | \gamma_1), F_1(x_2^* | \gamma_2), \dots, F_d(x_d^* | \gamma_d) | \theta))^T \quad (9)$$

$$197 \quad p_T^{AND} = 1 - (1 - \hat{C}(\bar{F}_1(x_1^* | \gamma_1), \bar{F}_2(x_2^* | \gamma_2), \dots, \bar{F}_d(x_d^* | \gamma_d) | \theta))^T \quad (10)$$

$$198 \quad p_T^{Kendall} = 1 - (P(C(F_1(x_1^* | \gamma_1), F_1(x_2^* | \gamma_2), \dots, F_d(x_d^* | \gamma_d) | \theta) \leq t))^T \quad (11)$$

199 where p_T^{OR} , p_T^{AND} , and $p_T^{Kendall}$ respectively denote the failure probability in “AND”,
 200 “OR” and “Kendall” cases. T indicate the service time of the facilities under
 201 consideration.

202
 203 Focusing on a bivariate case, the joint RP and the associate failure probability in
 204 “OR”, “AND”, and “Kendall” scenarios can be formulated as (Salvadori et al., 2007,
 205 2011; Graler et al., 2013; Sraj et al., 2014; Serinaldi, 2015):

$$206 \quad T_{u_1, u_2}^{OR} = \frac{\mu}{1 - C_{U_1 U_2}(u_1, u_2 | \theta)} \quad (12)$$

$$207 \quad T_{u_1, u_2}^{AND} = \frac{\mu}{1 - u_1 - u_2 + C_{U_1 U_2}(u_1, u_2 | \theta)} \quad (13)$$

$$208 \quad T_{u_1, u_2}^{Kendall} = \frac{\mu}{1 - P(C_{U_1 U_2}(u_1^*, u_2^*) \leq t)} \quad (14)$$

$$209 \quad p_T^{OR} = 1 - (C_{U_1 U_2}(u_1^*, u_2^* | \theta))^T \quad (15)$$

$$210 \quad p_T^{AND} = 1 - (u_1^* + u_2^* - \hat{C}_{U_1 U_2}(u_1^*, u_2^* | \theta))^T \quad (16)$$

1 211 $p_T^{Kendall} = 1 - (P(C_{U_1 U_2}(u_1^*, u_2^* | \theta) \leq t))^T$ (17)

2
3 212 where $u_1 = F_1(x_1 | \gamma_1), u_2 = F_2(x_2 | \gamma_2), u_1^* = F_1(x_1^* | \gamma_1), u_2^* = F_2(x_2^* | \gamma_2), (x_1^*, x_2^*)$

4
5 213 means the bivariate threshold.

6
7
8 214

9
10 215 **2.2. Uncertainty Quantification of Parameters by Bayesian Inference**

11
12 216

13
14 217 From Section 2.1, it is noticed that in the multivariate risk analysis framework
15
16 218 through copulas, parameters in both marginal distributions and copulas may produce
17
18 219 significant impacts on the resulting multivariate RPs and failure probabilities. In
19
20 220 particular, extensive uncertainties may be involved in the copula-based multivariate
21
22 221 risk assessment framework due to: (i) the inherent uncertainty in the flooding process,
23
24 222 (ii) uncertainty in the selection of appropriate marginal functions and copulas and (iii)
25
26 223 statistical uncertainty or parameter uncertainty within the parameter estimation
27
28 224 process (e.g. the availability of samples) (Serinaldi, 2013; Zhang et al., 2015). In this
29
30 225 study, the inherent uncertainty in the copula-based multivariate model will be
31
32 226 quantified by Bayesian analysis. The Bayesian approach has been widely applied for
33
34 227 uncertainty quantification since it can incorporate various sources of information into
35
36 228 a singly analysis through Bayes' theorem. Given the prior probability density and
37
38 229 observations, the posterior distribution can be derived through Bayes' theorem, which
39
40 230 is expressed as:

41
42
43 231
$$\pi(\theta | X) = \frac{L(\theta | X)\pi_0(\theta)}{\int L(\theta | X)\pi_0(\theta)d\theta}$$
 (18)

44
45
46
47 232

48
49 233 where $\pi_0(\theta)$ signifies the prior parameter distribution, and $L(\theta | X)$ denotes the
50
51 234 likelihood function. $\int L(\theta | X)\pi_0(\theta)d\theta$ is the normalization constant. $\pi(\theta | X)$ is the
52
53 235 posterior probability density function. $X = (x_1, x_2, \dots, x_d)$ is the observation vector.
54
55 236

56
57 237

58 237 Consider the multivariate distribution expressed by Equation (1), it is noticed that the
59
60 238 posterior distribution for the parameters in marginal distributions (i.e. $\gamma_i, i = 1, 2, \dots, d$)

61
62
63
64
65

239 and copula (i.e. θ) can be derived as follows:

$$\begin{aligned} 240 \quad & \pi(\gamma_1, \gamma_2, \dots, \theta | \mathbf{x}) \propto L(\gamma_1, \gamma_2, \dots, \theta | \mathbf{x}) \pi_0(\gamma_1, \gamma_2, \dots, \theta) \\ 241 \quad & = L(\gamma_1, \gamma_2, \dots, \theta | \mathbf{x}) \pi_0^1(\gamma_1) \pi_0^2(\gamma_2) \dots \pi_0^d(\gamma_d) \pi_0^c(\theta) \end{aligned} \quad (19)$$

242 where $L(\gamma_1, \gamma_2, \dots, \theta | \mathbf{x})$ is the likelihood function of the observation \mathbf{x} ($\mathbf{x} = x_1, x_2, \dots,$
243 x_d), $\pi_0^i(\gamma_i)$ are the prior distributions for parameters in marginal distribution, and
244 $\pi_0^c(\theta)$ indicates the prior for parameters in the copula.

245
246 For the probability distribution expressed by Equation (1), the corresponding
247 probability density function (PDF) can be derived as (Aas et al., 2009):

$$248 \quad f(x_1, \dots, x_d | \gamma_1, \dots, \gamma_d, \theta) = c(u_1, u_2, \dots, u_d | \theta) f_1(x_1 | \gamma_1) \dots f_d(x_d | \gamma_d) \quad (20)$$

249 where $c(\cdot)$ indicate the copula density, $f_i(\cdot)$ means the PDF of marginal distribution,
250 and $u_i = f_i(x_i | \gamma_i)$. Consequently, the likelihood function $L(\gamma_1, \gamma_2, \dots, \theta | \mathbf{x})$ can be
251 formulated as:

$$252 \quad L(\gamma_1, \gamma_2, \dots, \theta | \mathbf{x}) = \prod_{j=1}^n c(u_1^j, u_2^j, \dots, u_d^j | \theta) f_1(x_1^j | \gamma_1), \dots, f_d(x_d^j | \gamma_d) \quad (21)$$

253 where n is the total number of observations.

254
255 In spite of the likelihood function, the determination of prior distributions is an
256 essential step in any Bayesian analysis, as shown in Equations (18) and (19). The key
257 issues in setting up a priori distribution include (i) the information going into the prior
258 distribution; (ii) the properties of the resulting posterior distribution (Gelman, 2002).

259 In general, uninformative and informative priors are the two types of widely used
260 prior distributions, in which uninformative priors are adopted for the situation of no
261 information available for the prior and informative priors can provide some specific
262 information about the variable. However, with well-identified parameters and large
263 sample sizes, reasonable choices of prior distributions will have minor effects on
264 posterior inferences (Gelman, 2002). In this study, the normal informative priors are
265 assumed in terms of the parameters in marginal distribution and dependence structure.

266

267 In many situations, analytic solutions for Equation (18) are not possible. Thus, the
268 Markov chain Monte Carlo (MCMC) techniques are used to approximate sampling
269 realizations of the posterior distribution. A number of MCMC algorithms have been
270 proposed in both statistical and hydrological literatures. In this study, the
271 Metropolis-Hastings (MH) algorithm will be adopted for quantifying the posterior
272 distributions of the parameters in the copula-based multivariate hydrologic risk
273 framework. The MH algorithm, initially proposed by [Metropolis et al. \(1953\)](#) and
274 then extended by [Hastings \(1970\)](#), is widely used in hydrologic context (e.g. [Viglione
et al., 2013; Zhang et al., 2016](#)). In MH algorithm, a proposal density $q(\cdot)$ is used to
276 generate a new sample Θ' , given the current state Θ . Such a new sample is either
277 accepted or rejected through the Metropolis acceptance probability:

$$\alpha(\Theta, \Theta') = \min\left[\frac{q(\Theta | \Theta')\pi(\Theta' | \mathbf{x})}{q(\Theta' | \Theta)\pi(\Theta | \mathbf{x})}, 1\right] \quad (22)$$

279 where $\pi(\cdot)$ is the posterior distribution and $q(\cdot)$ is the proposal density function. Θ is the
280 parameters to be quantified. In this study, the parameters in both marginal
281 distributions and copulas are estimated simultaneously, and thus $\Theta = (\gamma_1, \gamma_2, \dots, \gamma_d, \theta)$.
282 Based on the sampling realizations from MCMC, the uncertainty and credibility
283 intervals can be analyzed. Also, the uncertainties in the resulting multivariate RP and
284 failure probabilities will be characterized.

285

286 In the copula-based multivariate risk assessment framework, there are several options
287 for both the marginal distributions (e.g. Lognormal, Pearson Type III, and generalized
288 extreme value distributions) and copula model (i.e. Gaussian, Archimedean copulas).
289 An essential step before inferencing hydrologic risk is to choose the most appropriate
290 model (i.e. marginal distribution and copula) to match the observed flood data. In this
291 study, the Deviance Information Criterion (DIC) will be employed to help choose the
292 most appropriate model. The index of DIC is developed by [Spiegelhalter et al. \(2002\)](#),
293 which is a specific measure designed for model selection under Bayesian inference
294 and can be thought of as a Bayesian alternative to the standard Akaike information

1
2
3
4
5
6
7
8
9
10
11
12
13
14
15
16
17
18
19
20
21
22
23
24
25
26
27
28
29
30
31
32
33
34
35
36
37
38
39
40
41
42
43
44
45
46
47
48
49
50
51
52
53
54
55
56
57
58
59
60
61
62
63
64
65

295 criterion (AIC) (Sarhadi et al., 2016). In the Bayesian inference through MCMC, the
296 DIC value can be formulated as (Spiegelhalter et al., 2002):

$$297 \quad DIC = D(\bar{\Theta}) + 2p_D \quad (23)$$

298 where

$$299 \quad D(\Theta) = -2 \log L(\text{data} | \Theta) \quad (24)$$

$$300 \quad p_D = \bar{D} - D(\bar{\Theta}) \quad (25)$$

301

302 **2.3. Uncertainty Partition through Multilevel Factorial Analysis**

303

304 Due to the uncertainties existing in the parameters in the copula-based multivariate
305 risk assessment model, the predictive risk (e.g. multivariate RP or failure probabilities)
306 values for a give hazardous event also present uncertain features. However, in the
307 copula-based multivariate risk assessment model, there are two kinds of parameters,
308 including the parameters in marginal distributions describing randomness of attributes
309 in the hazardous event and the parameters in copulas describing dependence
310 structures among attributes. Moreover, uncertainties in these parameters interact
311 among each other, leading to intensified uncertainty in predictive risk. Therefore,
312 multilevel factorial analysis will be used to characterize the contributions of
313 parameters in marginal distribution, copula and their interactions to the uncertainty in
314 the resulting risk inference values.

315

316 In factorial analysis, an experimental design is employed to account for all
317 combinations of the levels of factors to help visualize the single effects of factors with
318 discrete values (or levels) and their interactive effects on a response variable (Wang et
319 al., 2015). For instance, consider a copula-based bivariate risk assessment model
320 which has two marginal distributions (A and B) and one copula (C). The parameters in
321 the two marginal distributions are assumed to be respectively denoted as γ^A with a
322 levels and γ^B with b levels and the parameter in the copula is denoted with θ^C with c
323 levels. The predictive risk (denoted as R) of the copula model can be fitted in response

324 to the parameters $\gamma_A, \gamma_B, \theta_C$ and replicates n , which can be expressed as:

$$325 \quad R_{ijkl} = \mu + \theta_i^C + \gamma_j^A + \gamma_k^B + (\theta^C \gamma^A)_{ij} + (\theta^C \gamma^B)_{ik} + (\gamma^A \gamma^B)_{jk} + (\theta^C \gamma^A \gamma^B)_{ijk} + \varepsilon_{ijkl} \begin{cases} i = 1, 2, \dots, c \\ j = 1, 2, \dots, a \\ k = 1, 2, \dots, b \\ l = 1, 2, \dots, n \end{cases}$$

326 (26)

327 where μ denotes the overall mean effect; $\theta_i^C, \gamma_j^A, \gamma_k^B$ respectively indicate the effect
 328 for parameter θ^C in the copula at the i th level, parameter γ^A in the first marginal
 329 distribution at the j th level, and parameter γ^B in the first marginal distribution at the
 330 k th level; $(\theta^C \gamma^A)_{ij}, (\theta^C \gamma^B)_{ik}$ and $(\gamma^A \gamma^B)_{jk}$ indicate interactions between factors θ^C and
 331 γ^A, θ^C and γ^B , as well as γ^A and γ^B , respectively; $(\theta^C \gamma^A \gamma^B)_{ijk}$ denotes the interaction of
 332 factors θ^C, γ^A and γ^B ; ε_{ijkl} means the random error component.

333
 334 Based on Equation (26), the total variability of the predictive risk can be decomposed
 335 into its components parts as follows:

$$337 \quad SS_T = SS_{\theta^C} + SS_{\gamma^A} + SS_{\gamma^B} + SS_{\theta^C \gamma^A} + SS_{\theta^C \gamma^B} + SS_{\gamma^A \gamma^B} + SS_{\theta^C \gamma^A \gamma^B} + SS_e \quad (27)$$

338 and

$$339 \quad SS_T = \sum_{i=1}^c \sum_{j=1}^a \sum_{k=1}^b \sum_{l=1}^n R_{ijkl}^2 - \frac{R^2}{abcn} \quad (28)$$

$$340 \quad SS_{\theta^C} = \frac{1}{abn} \sum_{i=1}^c R_{i\dots}^2 - \frac{R^2}{abcn} \quad (29)$$

$$341 \quad SS_{\gamma^A} = \frac{1}{bcn} \sum_{j=1}^a R_{\cdot j \cdot \cdot}^2 - \frac{R^2}{abcn} \quad (30)$$

$$342 \quad SS_{\gamma^B} = \frac{1}{acn} \sum_{k=1}^b R_{\cdot \cdot k \cdot}^2 - \frac{R^2}{abcn} \quad (31)$$

$$343 \quad SS_{\theta^C \gamma^A} = \frac{1}{bn} \sum_{i=1}^c \sum_{j=1}^a R_{ij \cdot \cdot}^2 - \frac{R^2}{abcn} - SS_{\theta^C} - SS_{\gamma^A} \quad (32)$$

$$344 \quad SS_{\theta^c \gamma^B} = \frac{1}{an} \sum_{i=1}^c \sum_{k=1}^b R_{i.k.}^2 - \frac{R_{\dots}^2}{abcn} - SS_{\theta^c} - SS_{\gamma^B} \quad (33)$$

$$345 \quad SS_{\gamma^A \gamma^B} = \frac{1}{cn} \sum_{j=1}^a \sum_{k=1}^b R_{.jk.}^2 - \frac{R_{\dots}^2}{abcn} - SS_{\gamma^A} - SS_{\gamma^B} \quad (34)$$

$$346 \quad SS_{\theta^c \gamma^A \gamma^B} = \frac{1}{n} \sum_{i=1}^c \sum_{j=1}^a \sum_{k=1}^b R_{ijk.}^2 - \frac{R_{\dots}^2}{abcn} - SS_{\theta^c} - SS_{\gamma^A} - SS_{\gamma^B} - SS_{\theta^c \gamma^A} - SS_{\theta^c \gamma^B} - SS_{\gamma^A \gamma^B} \quad (35)$$

$$347 \quad SS_e = \sum_{i=1}^c \sum_{j=1}^a \sum_{k=1}^b \sum_{l=1}^n R_{ijkl}^2 - \frac{1}{n} \sum_{i=1}^c \sum_{j=1}^a \sum_{k=1}^b R_{ijk.}^2 \quad (36)$$

348

$$349 \quad \text{where } R_{ijk.} = \sum_{l=1}^n R_{ijkl}, R_{ij..} = \sum_{k=1}^b \sum_{l=1}^n R_{ijkl}, R_{.jk.} = \sum_{i=1}^c \sum_{l=1}^n R_{ijkl}, R_{i.k.} = \sum_{j=1}^a \sum_{l=1}^n R_{ijkl},$$

$$350 \quad R_{i...} = \sum_{j=1}^a \sum_{k=1}^b \sum_{l=1}^n R_{ijkl}, R_{.j..} = \sum_{i=1}^c \sum_{k=1}^b \sum_{l=1}^n R_{ijkl}, R_{..k.} = \sum_{i=1}^c \sum_{j=1}^a \sum_{l=1}^n R_{ijkl}$$

$$351 \quad R_{\dots} = \sum_{i=1}^c \sum_{j=1}^a \sum_{k=1}^b \sum_{l=1}^n R_{ijkl}. \text{ Then the contributions of parameter uncertainties in}$$

352 marginal distributions and dependence structures can be calculated as:

353 (1) Contributions of parameters in marginal distributions A and B

$$354 \quad \eta_A = SS_{\gamma^A} / SS_T \quad (37)$$

$$355 \quad \eta_B = SS_{\gamma^B} / SS_T \quad (38)$$

356 (2) Contribution of parameter in the dependence structure

$$357 \quad \eta_C = SS_{\theta^c} / SS_T \quad (39)$$

358 (3) Contributions of parameter interactions

$$359 \quad \eta_{AC} = SS_{\theta^c \gamma^A} / SS_T \quad (40)$$

$$360 \quad \eta_{BC} = SS_{\theta^c \gamma^B} / SS_T \quad (41)$$

$$361 \quad \eta_{AB} = SS_{\gamma^A \gamma^B} / SS_T \quad (42)$$

$$362 \quad \eta_{ABC} = SS_{\theta^c \gamma^A \gamma^B} / SS_T \quad (43)$$

363 (4) Contribution of internal variability

$$364 \quad \eta_e = SS_e / SS_T \quad (44)$$

365

1 366 **3. Applications**

2 367

3 368 The proposed FBC approach is applied for hydrologic risk analysis at three locations

4 369 in China, one at the Xingxi River and two at the Wei River. The detailed descriptions

5 370 for these two catchments are provided in the [Supplementary Materials](#). Observed

6 371 daily streamflow data Xingshan station (at Xiangxi River) and Xianyang and

7 372 Zhangjiashan gauging stations (at Wei River) are applied for hydrologic risk analysis.

8 373 [Figure 2](#) show the locations of these three gauging stations. Although a flood is

9 374 generally characterized by its peak, volume and duration, the multivariate flood risk in

10 375 terms of peak and volume will be applied to demonstrate the applicability for the

11 376 proposed FBC method. Other multivariate risk indices for peak-duration,

12 377 volume-duration and peak-volume-duration can similarly be characterized by the

13 378 developed FBC method. Based on the daily stream flow data, the flood peak applied

14 379 is defined as the maximum daily flow over a period and the associated flood volume

15 380 is considered as the cumulative flow during the flood period. In current study, the

16 381 flood characteristics are obtained based on the annual scale. This means that one flood

17 382 event is identified in one year. The detailed method to identify the flood peak and the

18 383 associated flood volume can be found in studies by [Yue \(2000, 2001\)](#). [Table 1](#) shows

19 384 some descriptive statistics values of the considered variables (peak discharge, Q ;

20 385 hydrograph volume, V). In detail, the daily discharge data from 1961 to 2010 are used

21 386 to analyze the potential flooding risk in Xiangxi River, which means 50 flood peak

22 387 and volume values (i.e. one flood peak and volume in each year) are generated.

23 388 Similarly, 47 and 55 flood events are characterized at the Xianyang and Zhangjiashan

24 389 station, respectively.

25 390

26 391 -----

27 392 Place Figure 2 and Table 1 here

28 393 -----

29 394

30 395 **4. Results Analysis**

31

32

33

34

35

36

37

38

39

40

41

42

43

44

45

46

47

48

49

50

51

52

53

54

55

56

57

58

59

60

61

62

63

64

65

4.1. Parameter Estimation and Model Selection

There are a number of potential models for both marginal distributions and dependent structures. In this study, three models including generalized extreme value (GEV), lognormal (LN) and Pearson Type III (PIII) distributions are selected to fit the distributional characteristics of flood peak and volume at the Xingshan, Zhangjiashan and Xianyang stations. Meanwhile, three Archimedean copulas involving Joe, Gumbel and Frank copula are applied to reflect the dependence structure between those two flood attributes (i.e. peak and volume). The parameters in both marginal distributions and copula are quantified through MH-based MCMC approach and the most appropriate model is determined by the values of DIC.

For each gauge station, the combinations of marginal distributions and copula functions will lead to a total number of 27 potential risk assessment models. For each model, the MH-based MCMC algorithm is run for 50,000 iterations in which the first 30% samples are neglected as burn-in and the rest ones are used to quantify the posterior distributions of model parameters. The Geweke's diagnostic is applied to guarantee the convergence of the Markov chain for each parameter (the absolute value of test statistic is less than 1.96) (Plummer et al., 2015). The associated DIC values are calculated based on the posterior samples in which the model with a minimum DIC value is chosen as the most appropriate one for further risk inference.

Table 2 presents the results for model selection for the three streamflow gauge stations (i.e. Xingshan, Zhangjiashan and Xianyang). The results indicate that for each flood attribute (i.e. peak and volume), the lognormal distribution will be applied to quantify its distributional characteristic. In particular, the lognormal distribution will be used for all the two flood attributes at all three gauge stations. In terms of the dependence structure between flood peak and volume, the Gumbel copula will be used for the Xiangxi River (i.e. Xingshan station), while the Frank copula is chosen for Wei River (i.e. Zhangjiashan and Xianyang stations). Figure 3 shows the posterior

1
2
3
4
5
6
7
8
9
10
11
12
13
14
15
16
17
18
19
20
21
22
23
24
25
26
27
28
29
30
31
32
33
34
35
36
37
38
39
40
41
42
43
44
45
46
47
48
49
50
51
52
53
54
55
56
57
58
59
60
61
62
63
64
65

426 distributions for the parameters in the copula-based risk assessment model at the three
427 gauge stations. The first row indicates the parameter posteriors for the lognormal
428 distribution models for flood peak at the three stations while the second row presents
429 the posterior distributions for the flood volume models. The last row in Figure 3
430 shows the parameter posteriors in the copula functions. The results in Figure 3 suggest
431 that the uncertainty in model parameters can be well reflected by the MCMC
432 algorithm with relative small deviations. Such results can also be demonstrated by the
433 95% predictive intervals (PIs) for each parameter as presented in Table 2.

434 -----

436 Place Figure 3 and Table 2 here

437 -----

439 **4.2. Uncertainty in Risk Inferences**

440
441 Parameter uncertainties in both marginal distributions and the dependence structure
442 will also lead to uncertainty in the risk inference results. [Figure 4](#) describes the
443 inferred flood peak and volume generated based on the lognormal model. Since
444 parameters in all lognormal models have some degrees of uncertainty (as shown in
445 [Figure 3](#) and [Table 2](#)), the inferred flood peak and volume values with specific return
446 periods exhibit obvious uncertainties. Particularly, these uncertainties would be more
447 extensive as the increase in the predefined return period.

448 -----

450 Place Figure 4 here

451 -----

452
453
454 In addition to uncertainties in predictive flood peak and volume, parameter
455 uncertainties in both marginal distributions and the copula function also lead to
456 imprecise values for joint risks of peak and volume. [Figure 5](#) describes uncertainties

1 457 for joint RP in OR at the three stations. It is observed that the predictive joint RP in
2 458 OR has small uncertainty for a small flood event (i.e. small peak or small volume),
3
4 459 while considerable uncertainties exist in the predictive joint RP of OR even for a
5
6 460 flood with an actual joint RP of 20 years. For the predictive joint RP in AND, more
7
8 461 extensive uncertainties exist than that for the joint RP in OR, as shown in [Figure S1 in](#)
9
10 462 [the Supplementary Materials](#). Noticeable uncertainties exist in the predictive joint RP
11
12 463 of AND even for a minor flood event with a 5-year joint RP of AND. For some
13
14 464 extreme flood events (e.g. with a 200-year joint RP of AND), the predictive joint RP
15
16 465 in AND can be remarkably large. For the joint RP in Kendall, the uncertainties in the
17
18 466 predictive values are not as remarkable as those for joint RP in AND, as presented in
19
20 467 [Figure S2 in the Supplementary Materials](#). However those uncertainties are still
21
22 468 noticeable even for a moderate flood event with a 50-year joint RP in Kendall.
23
24
25 469
26
27 470 -----
28
29 471 Place Figures 5 here
30
31 472 -----
32
33 473

34 474 In additional to the joint RP in AND, OR and Kendall, the FP provides more
35
36 475 consistent way for multivariate hydrological or environmental risks ([Serinaldi, 2015;](#)
37
38 476 [Salvador et al., 2016](#)). The formulations for calculating these FPs are expressed by
39
40 477 Equations (9) – (11) and Equations (15) – (17). In this study, the critical thresholds for
41
42 478 flood peak and volume are inferred based on their corresponding probability
43
44 479 distributions with a predefined return period of 500 (i.e. $p = 0.998$) and the service
45
46 480 time of one hydraulic infrastructure (e.g. a dam or river levee) ranges from 30 to 100
47
48 481 years. The associated FPs in OR, AND and Kendall, corresponding to the above
49
50 482 critical peak and volume thresholds as well as service time scenarios, are shown in
51
52 483 [Figure 6](#). It is observed that, as a result of uncertain parameters in both marginal
53
54 484 distributions and the dependence structure, noticeable uncertainties exist in the
55
56 485 predictive FPs of OR, AND and Kendall. More specifically, the degree of uncertain of
57
58 486 FPs would increase significantly if the service time of one hydraulic infrastructure
59
60
61
62
63
64
65

1 487 increases.

2 488

3 489 -----

4 490 Place Figure 6 here

5 491 -----

6 492

7 493 **4.3. Interactions of parameter uncertainties**

8 494

9 495 Great uncertainties exist in the inferred risk values (i.e. joint RP and FPs) due to
10 496 imprecise estimations for the parameters in the copula-based risk assessment model.
11 497 However, one unclear issue is that how the parameter uncertainties and their
12 498 interactions impact the risk inference of the copula-based risk model. Therefore, a
13 499 multilevel factorial design (expressed as Equations (26) – (36)) is proposed to
14 500 characterize the main and interactive effects of parameters in marginal distributions
15 501 and copula function on the resulting risk inference values. In detail, a 3^5 factorial
16 502 design is proposed in which the five parameters considered as the factors, in which
17 503 two of them (denoted as P_par1 , P_par2) are the parameters in the lognormal
18 504 distribution for flood peak, two (denoted as V_par1 , V_par2) are the parameters in the
19 505 lognormal distribution for flood volume, and the last one is the parameter (i.e.
20 506 Cop_par) in the copula function. Each factor has three levels (i.e. 0.05, 0.5, and 0.95)
21 507 identifies as the 5%, 50% and 95% quantiles of its posterior samples from MCMC.
22 508 Three responses are considered in the factorial design, which are corresponds to the
23 509 three failure probabilities (i.e. OR, AND, and Kendall). A multi-way analysis of
24 510 variance (ANOVA) is further employed to identify the statistical significance of all
25 511 parameters and their interactions in the copula-based risk assessment model.

26 512

27 513 **Figure 7** presents the main effect plots and full interactions plot matrices for
28 514 parameters on the FP in OR at Xingshan, Xianyang and Zhangjiashan stations. It is
29 515 noticed that both the main effect plots and the interaction plot matrices at the three
30 516 stations have similar patterns, implying that the parameters' individual and interactive

1
2
3
4
5
6
7
8
9
10
11
12
13
14
15
16
17
18
19
20
21
22
23
24
25
26
27
28
29
30
31
32
33
34
35
36
37
38
39
40
41
42
43
44
45
46
47
48
49
50
51
52
53
54
55
56
57
58
59
60
61
62
63
64
65

1 517 effects on the FP are nearly independent with the location of one gauge station. More
2 518 specifically, the changes of the two scale parameters (i.e. P_{par2} and V_{par2}) lead to
3 519 more changes in response (i.e. FP in OR) than the changes of the two location
4 520 parameters (i.e. P_{par1} and V_{par2}). This indicates that the scale parameter in
5 521 lognormal distribution has a more effect on the inferred FP of OR than the location
6 522 parameter. Moreover, the resulting failure probability does not have a visible change
7 523 as the copula parameter change from its low level to its high level, suggesting that the
8 524 parameter in the copula function may has insignificant effect on the prediction of
9 525 failure probability in OR. For the interactive effects among the five parameters, the
10 526 full interactions plot matrices show that the interactive curves between the copula
11 527 parameter (i.e. Cop_{par}) and the location parameter of peak (i.e. P_{par1}) are parallel
12 528 at the three levels, indicating an insignificant interaction of these two parameters on
13 529 the inferred failure probability of OR. Similar characteristics are also observed for the
14 530 interactions between the copula parameter and the other three parameters (i.e. P_{par2} ,
15 531 V_{par1} , V_{par2}). Other interactive curves are observed to be intersected at the three
16 532 levels, implying significant interactive effects of those parameters on the results risk
17 533 inference. [Table 3](#) provides the results of ANOVA table for the failure probability in
18 534 OR. The results indicate statistical insignificance for AE, BE, CE and DE, which is
19 535 consistent with the full interaction plot matrices. The individual effect of the copula
20 536 parameter (i.e. Cop_{par}) is statistical insignificant at the Xianyang and Zhangjiashan
21 537 stations, while such an effect is statistical significant at the Xingshan station. However,
22 538 this parameter leads to less sum of squares than the other four parameters at all three
23 539 cases, implying a least main effect among those five parameters, which is also
24 540 observed from Figure 7.

25 541

26 542 -----

27 543 Place Figure 7 and Table 3 here

28 544 -----

29 545

30 546 In terms of the FP in AND, the results in [Figure S3 in the Supplementary Materials](#)

1
2
3
4
5
6
7
8
9
10
11
12
13
14
15
16
17
18
19
20
21
22
23
24
25
26
27
28
29
30
31
32
33
34
35
36
37
38
39
40
41
42
43
44
45
46
47
48
49
50
51
52
53
54
55
56
57
58
59
60
61
62
63
64
65

1 547 indicate that both individual effects of the parameters and their interactions have
2 548 similar features for all three stations, which is also observed in [Figure 7](#). Also, for the
3
4 549 individual effects, the two scale parameters (i.e. P_{par2} and V_{par2}) lead to steeper
5
6 550 lines than the lines corresponding to the two location parameters (i.e. P_{par1} and
7
8 551 V_{par1}), suggesting more significant effects of the scale parameters than those from
9
10 552 the location parameters. It is also noticed that among the five parameters, the copula
11
12 553 parameter (i.e. Cop_{par}) contributes least individual effects on the variation of FP in
13
14 554 AND. Furthermore, significant interactive effects are observed among the parameters
15
16 555 in the two marginal distributions (i.e. P_{par1} , P_{par2} , V_{par1} , and V_{par2}) which
17
18 556 are indicated by intersecting lines in [Figure S3](#). Some interactions also occur between
19
20 557 the copula parameter and the parameters in marginal distributions, which are different
21
22 558 from those for the FP in OR described in [Figure 7](#). These interactions may probably
23
24 559 because that, besides the joint probability values, the cumulative probabilities of flood
25
26 560 peak and volume are also used to derive the FP in AND (i.e. Equations (10) and (16)).
27
28 561 This leads to more chances for occurrence of visible interactions between the copula
29
30 562 parameter and others. The above findings can be further demonstrated by the results
31
32 563 of ANOVA for failure probability in AND. As presented in [Table S1 in the](#)
33
34 564 [Supplementary Materials](#), the copula parameter results into least sum of squares,
35
36 565 suggesting least individual effects among the five parameters. Also, statistical
37
38 566 significance for parameter interactions can be observed except to the interactions of
39
40 567 AE and CE.
41
42 568
43
44 569 [Figure S4 in the Supplementary Materials](#) presents the main effects plot and full
45
46 570 interactions plot matrices for parameters on the FP in Kendall at the three gauge
47
48 571 stations, and [Table S2](#) gives the associate ANOVA results. It can be found that the
49
50 572 results of failure probability in Kendall have similar characteristics at the three sites,
51
52 573 which are also found for the previous two failure probabilities (i.e. AND, OR). Also,
53
54 574 the copula parameter results into least sloped curve and least sum of squares, implying
55
56 575 least main effect on the inferred failure probability in Kendall. For the interactive
57
58 576 effects among the five parameters, intersection lines are observed for all pairs of
59
60
61
62
63
64
65

1 577 parameters, suggesting apparent interactive effects, which are also demonstrated by
2 578 the ANOVE results in Table S2.

3 579 4 580 **4.3 Contributions of Uncertainty Sources** 5 581

6 582 In the copula-based risk assessment model, parameters in marginal distributions pose
7 583 significant individual and interactive effects on the inferred failure probabilities, while
8 584 the parameter in the copula function has least main effects (e.g. statistical
9 585 insignificance in some cases) and the interactions for this parameter and others are
10 586 sometime insignificant. As a result of parameter uncertainties, the predictive failure
11 587 probabilities exhibit noticeable uncertainties as shown in [Figure 6](#). Such uncertainties
12 588 become more significant with the increase in service time. However, two more issues
13 589 to be explored are that (i) how much these parameters contribute to the variation of
14 590 the inferred risk values and (ii) do these contributions change significantly for the
15 591 failure probabilities with different service time scenarios. Consequently, further
16 592 multi-level factorial analysis is conducted in response to failure probabilities with
17 593 multiple service time scenarios in order to identify (i) the contributions of parameters
18 594 and their interactions on the variations or uncertainties in predictive failure
19 595 probabilities, and (ii) how these contributions change with the variation in service
20 596 time. In detail, to get more reliable quantification, five levels are considered for each
21 597 parameter which is identified as 5%, 25%, 50%, 75% and 95% quantiles of the
22 598 parameter's posterior samples. Four service time scenarios, namely 30, 50, 70, and
23 599 100 years, are under consideration to answer the change of one contribution with
24 600 varied service time scenario. Moreover, only a single replicate is conducted for the
25 601 factorial analysis, in which three and higher-way interactions are combined to give an
26 602 estimate of internal error in the associated ANOVA. Finally, the contributions of
27 603 parameters in marginal distributions and copula are characterized based on Equations
28 604 (37) – (39), and the interactive effects of these parameters are combined together by
29 605 summing results of Equations (40) – (44).

30 606
31 607 [Figure 8](#) shows detailed contributions of model parameters on uncertainty in
32
33
34
35
36
37
38
39
40
41
42
43
44
45
46
47
48
49
50
51
52
53
54
55
56
57
58
59
60
61
62
63
64
65

1 608 predictive failure probabilities of OR at Xingshan, Xianyang and Zhangjiashan
2 609 stations. It can be observed that, even though some discrepancies exist for
3 610 contributions of model parameters at different stations, the results show similar
4 611 features, in which the scale parameters (i.e. P_{par2} , and V_{par2}) give more
5 612 contributions (larger than 25%) in risk inference than of the location parameters (i.e.
6 613 P_{par1} and V_{par1}), and the parameter in copula function pose least impact (less
7 614 than 1%). However, in terms of the interaction of model parameters, parameter
8 615 interactions provide more impact (more than 14%) at the Xiangshan station than that
9 616 (less than 8%) at the Xianyang and Zhangjiashan stations. This may be probably
10 617 because that the Xingshan station is located in the Xingxi River basin with a northern
11 618 subtropics climate while the Xianyang and Zhangjiashan stations are located Wei
12 619 River basin experienced a semi-arid and sub-humid continental monsoon climate.
13 620 Moreover, the detailed contribution of one parameter would not change significantly
14 621 for different service time scenarios. For instance, as the service time changes from 30
15 622 to 100 years, the contribution of P_{par1} at Xingshan station ranges from 7.93% to
16 623 8.42%.

17 624
18 625 For the failure probability in AND, the parameters in marginal distributions and the
19 626 copula function have different effects with those parameters' impacts on the failure
20 627 probability in OR. As presented in [Figure S5 in the Supplementary Materials](#), the
21 628 scale parameters (i.e. i.e. P_{par2} , and V_{par2}) in marginal distributions also pose
22 629 significant impacts on uncertainties in the failure probabilities in AND. However, the
23 630 detailed contributions are less than those parameters on the failure probabilities in OR
24 631 shown in [Figure 8](#). For instance, the scale parameters contribute 30.51% and 26.91%
25 632 respectively to the predictive uncertainty in failure probability in AND with a service
26 633 time of 30-year at Xingshan Station, while these two parameters give contributions of
27 634 39% and 28.56% respectively for the failure probability in OR. Such decreases of
28 635 individual effects of scale parameters are mainly due to the remarkable increasing
29 636 effects of interactions, which increase from about 15% to more than 25% at Xingshan
30 637 station and from less than 10% to more than 30% at Xianyang and Zhangjishan

1 638 stations. The significant increase of the interactive effect also leads to visible decrease
2 639 in the contributions of location parameters (i.e. P_{par1} and V_{par1}). The
3
4 640 contributions of the copula parameter are still neglectable even though they increase
5
6 641 slightly from less than 0.1% for failure probabilities in OR to about 1% for the failure
7
8 642 probabilities in AND.
9

10 643
11
12 644 For the uncertainty partition in the failure probability of Kendall, it can be noticed
13
14 645 from [Figure S6 in the Supplementary Materials](#) that the scale parameters have most
15
16 646 significant contributions on the failure probabilities in Kendall, followed by the
17
18 647 interaction of model parameters, the location parameters, and the copula parameter.
19
20 648 Moreover, such contribution partition does not change explicitly in response to the
21
22 649 change in service time scenarios. However, compared with parameters' contributions
23
24 650 to the failure probabilities in OR and AND, the contributions of parameters in
25
26 651 marginal distributions (i.e. P_{par1} , P_{par2} , V_{par1} , and V_{par2}) to the failure
27
28 652 probabilities of Kendall are generally larger than those contributions to failure
29
30 653 probability in AND but less than the contributions to failure probability in OR. In
31
32 654 comparison, the contribution of parameters' interaction to the failure probability in
33
34 655 Kendall is less than the contribution to the failure probability in AND but larger than
35
36 656 its contribution to the failure probability in OR. This is probably due to the differences
37
38 657 in calculation of failure probabilities in OR, AND, and Kendall (i.e. Equations (9) –
39
40 658 (11) and Equations (15) – (17)), in which parameters' interaction has more chance to
41
42 659 pose a significant impact on the variations of the inferred risks in OR and AND than
43
44 660 the risk in OR.
45
46
47
48
49

50 662 **5. Conclusions**

51
52 663
53
54 664 In this study, a factorial Bayesian copula (FBC) approach has been proposed to
55
56 665 quantify parameters' uncertainties, reveal individual and interactive effects of
57
58 666 parameters and further characterize contributions of these parameters on the inferred
59
60
61
62
63
64
65

1 667 risk values. The developed FBC approach integrates copula-based risk assessment
2 668 model, Bayesian inference and factorial analysis into a general framework. In detail, a
3
4 669 Bayesian-based Markov chain Monte Carlo approach is employed to quantify
5
6 670 parameter uncertainties in the copula-based risk inference model; multi-level factorial
7
8 671 analysis is proposed to reveal individual and interactive effects of model parameters
9
10 672 on risk inference, and the associated analysis of variance (ANOVA) is further
11
12 673 proposed to identify the contributions of model parameters and their interaction on the
13
14 674 predictive risk values.
15

16 675
17
18 676 To illustrate the applicability of the proposed FBC approach, flood observations at
19
20 677 three gauge stations have been used to reveal parameters' uncertainty and their
21
22 678 contributions to the joint risk of flood peak and volume. The joint RPs and the
23
24 679 associated FPs in OR, AND and Kendall are considered as the risks of interest. Based
25
26 680 on those case studies, some findings can be concluded:
27

- 28 681 1. Parameter uncertainty is one of the unavoidable factors to be well identified in
29
30 682 multivariate risk analysis, and imprecise parameters in copula-based models can lead
31
32 683 to great uncertainties in all inferred joint RPs and FPs in OR, AND and Kendall.
33
34 684 2. For different risk indices, the main and individual effects of parameters have some
35
36 685 different features. In general, the scale parameters in the lognormal distributions of
37
38 686 peak and volume have more individual effects than the location parameters for all
39
40 687 three failure probabilities, followed by the location parameters and the parameter in
41
42 688 copula function. But all interactive effects of the copula parameter and other
43
44 689 parameters in marginal distributions are generally statistical insignificant for the FP in
45
46 690 OR, while some of them are statistical insignificant for the FP in AND, and all of
47
48 691 them are significant for the FP in Kendall. Moreover, such features are almost
49
50 692 independent with the location of a gauge station.
51
52 693 3. For the detailed contributions, parameters in marginal distributions of peak and
53
54 694 volume pose most contributions for the FP in OR, followed by their contributions to
55
56 695 FPs in Kendall and AND. In contrast, the parameters' interaction has a more impact
57
58 696 for FP in AND than its contributions to Kendall and OR. The copula parameter has
59
60
61
62
63
64
65

1 697 least contributions for all three FPs even through it increases from less than 0.1% to
2 698 about 2% for FPs of OR to Kendall. The above contribution characterization does not
3
4 699 change visibly for FPs with different service time scenarios.
5

6 700

7
8 701 The presence of uncertainties would pose significant impact on risk inferences within
9
10 702 both univariate and multivariate contexts. Many studies have been reported to
11
12 703 quantify uncertainties in hydrological risk analysis (e.g. [Serinaldi, 2013](#); [Zhang et al.,](#)
13
14 704 [2015](#); [Dung et al., 2015](#); [Fan et al., 2018](#)). However, as an extension of previous
15
16 705 studies, the major contributions in this study is that the proposed FBC method cannot
17
18 706 effectively quantify parameter uncertainties in the copula-based multivariate risk
19
20
21 707 inference model, but also characterize the individual and interactive effects of those
22
23 708 uncertainties on the resulting risk inferences. Also, the develop FBC approach can
24
25 709 help track the major contributors (e.g. parameter uncertainties in marginal
26
27 710 distributions) to the resulting uncertainties in risk inferences. Such results would be
28
29 711 helpful to find potential pathways for uncertainty reduction in hydrological risk
30
31 712 inferences.
32

33 713

34
35 714 The applicability of FBC has been illustrated through multivariate flood risk inference
36
37 715 under consideration of the dependence between flood peak and volume. Nevertheless,
38
39 716 this method can also be applied for other risk assessment issues such the compound
40
41 717 hydroclimatic extremes (e.g. drought and heat waves ([Sun et al., 2019](#)), soil moisture
42
43 718 and precipitation ([AghaKouchak, 2015](#))), water quality ([Shi and Xia, 2017](#)), air
44
45 719 pollution ([Sak et al., 2017](#)), and so on.
46

47 720

48 721 **Acknowledgement**

49
50 722 This research was supported by the National Key Research and Development Plan
51
52 723 (2016YFC0502800, 2016YFA0601502), the Natural Sciences Foundation of China
53
54 724 (51190095, 51225904), and the Natural Science and Engineering Research Council of
55
56 725 Canada.
57

58 726

59
60
61
62
63
64
65

727 **Appendix A. Abbreviation**

| | |
|-------|---|
| AIC | Akaike information criterion |
| AND | All elements in the extreme events should exceed the corresponding thresholds |
| ANOVA | Analysis of variance |
| FBC | Factorial Bayesian copula |
| DIC | Deviance Information Criterion |
| FP | Failure probabilities |
| GEV | Generalized extreme value distribution |
| LN | Lognormal distribution |
| MCMC | Markov chain Monte Carlo |
| MH | Metropolis-Hastings algorithm |
| OR | At least one element surpass the predefined threshold |
| PDF | Probability density function |
| PI | Predictive interval |
| PIII | Pearson Type III distribution |
| RP | Return period |
| TGR | Three Gorges Reservoir |

728

729

1
2
3
4
5
6
7
8
9
10
11
12
13
14
15
16
17
18
19
20
21
22
23
24
25
26
27
28
29
30
31
32
33
34
35
36
37
38
39
40
41
42
43
44
45
46
47
48
49
50
51
52
53
54
55
56
57
58
59
60
61
62
63
64
65

730 **References**

- 731 Aas, K., C. Czado, A. Frigessi, and H. Bakken (2009), Pair-copula constructions of multiple
732 dependence, *Insurance: Mathematics and Economics*, 44, 182–198.
- 733 AghaKouchak, A. (2015), A multivariate approach for persistence-based drought prediction:
734 Application to the 2010–2011 East Africa drought, *Journal of Hydrology*, 526, 127–135
- 735 Chebana F., and Ouarda T.B.M., (2011). Multivariate quantiles in hydrological frequency analysis.
736 *Environmetrics*, 22(1), 63-78.
- 737 De Michele C, Salvadori G (2003) A Generalized Pareto intensity-duration model of storm rainfall
738 exploiting 2-copulas. *Journal of Geophysical Research*, 108(D2), 4067,
739 doi:10.1029/2002JD002534.
- 740 Dung N.V., Merz B., Bardossy A., Apel H., (2015). Handling uncertainty in bivariate quantile
741 estimation – An application to flood hazard analysis in the Mekong Delta. *Journal of Hydrology*,
742 527, 704-717.
- 743 Fan Y.R., Huang W.W., Huang G.H., Huang K., Zhou X., (2015a). A PCM-based stochastic
744 hydrologic model for uncertainty quantification in watershed systems. *Stochastic*
745 *Environmental Research and Risk Assessment*, 29(3) 915-927.
- 746 Fan Y.R., Huang W.W., Li Y.P., Huang G.H., Huang K., (2015b). A coupled ensemble filtering and
747 probabilistic collocation approach for uncertainty quantification of hydrological models. *Journal*
748 *of Hydrology*, 530, 255-272.
- 749 Fan Y.R., G.H., Huang, K., Huang, (2018). Uncertainty Analysis for Multivariate Hydrologic Risk
750 in the Xiangxi River in Three Gorges Reservoir Area, China, *Engineering*, 4(5), 617-626.
- 751 Fan Y.R., Huang W.W., Huang G.H., Huang K., Li Y.P., Kong X.M., (2016a). Bivariate hydrologic
752 risk analysis based on a coupled entropy-copula method for the Xiangxi River in the Three
753 Gorges Reservoir area, China, *125 (1-2)*, 381-397
- 754 Fan Y.R., Huang W.W., Huang G.H., Li Y.P., Huang K., (2016b). Hydrologic Risk Analysis in the
755 Yangtze River basin through Coupling Gaussian Mixtures into Copulas. *Advances in Water*
756 *Resources*, 88, 170-185.
- 757 Fan Y.R., Huang G.H., Baetz B.W., Li Y.P., Huang K., (2017). Development of a Copula - based
758 Particle Filter (CopPF) Approach for Hydrologic Data Assimilation under Consideration of
759 Parameter Interdependence. *Water Resources Research*, 53(6), 4850-4875.
- 760 Favre, A.-C., S. El Adlouni, L. Perreault, N. Thiémondge, and B. Bobée (2004), Multivariate
761 hydrological frequency analysis using copulas, *Water Resources Research* 40, W01101,
762 doi:10.1029/2003WR002456
- 763 Gelman A., Prior distribution. In: Abdel H. El-Shaarawi and Walter W. Piegorsch, editors
764 *Encyclopedia of Environmetrics*, John Wiley & Sons, Vol. 3,2002, p. 1634–1637.
- 765 Genest C, Favre AC. (2007). Everything you always wanted to know about copula modeling but
766 were afraid to ask. *Journal of Hydrologic Engineering*, 12(4): 347–368.

1
2
3
4
5
6
7
8
9
10
11
12
13
14
15
16
17
18
19
20
21
22
23
24
25
26
27
28
29
30
31
32
33
34
35
36
37
38
39
40
41
42
43
44
45
46
47
48
49
50
51
52
53
54
55
56
57
58
59
60
61
62
63
64
65

767 Graler B., van den Berg M.J., Vandenberghe S., Petroselli A., Grimaldi S., De Baets B., Verhoest
768 N.E.C., (2013). Multivariate return periods in hydrology: a critical and practical review
769 focusing on synthetic design hydrograph estimation. *Hydrology and Earth System Sciences* 17:
770 1281–1296.

771 Hastings, W.K., 1970. Monte Carlo sampling methods using Markov chains and their application.
772 *Biometrika* 57, 97–109.

773 Huang K., Dai L.M., Yao M., Fan Y.R., Kong X.M., (2017). Modelling dependence between
774 traffic noise and traffic flow through an entropy-copula method, *Journal of Environmental*
775 *Informatics*, 29(2), 134 – 151, doi:10.3808/jei.201500302

776 Huang G.W., Liu H., Li X., and Ma M., (2019). Exploring Drivers of Nitrate Contamination of
777 Drinking Water in an Arid Region of China. *Journal of Environmental Informatics*, 32(2),
778 105-112.

779 Joe, H. (2014), *Dependence Modeling With Copulas*, Chapman and Hall, London, U. K.

780 Kao S.C., Govindaraju R.S., (2010). A copula-based joint deficit index for droughts. *Journal of*
781 *Hydrology*, 380, 121-134.

782 Karmakar S., Simonovic S.P., (2009). Bivariate flood frequency analysis. Part 2: a copula-based
783 approach with mixed marginal distributions. *Journal of Flood Risk Management*, 2, 32-44.

784 Kidson R., Richards K.S., (2005). Flood frequency analysis: assumption and alternatives. *Progress*
785 *in Physical Geography*, 29(3), 392-410.

786 Kong X.M., Huang G.H., Fan Y.R., Li Y.P., (2015). Maximum entropy-Gumbel-Hougaard copula
787 method for simulation of monthly streamflow in Xiangxi river, China. *Stochastic*
788 *Environmental Research and Risk Assessment*, 29, 833-846

789 Lee T, Salas JD. 2011. Copula-based stochastic simulation of hydrological data applied to Nile
790 River flows. *Hydrology Research* 42(4): 318–330.

791 Li Z., Huang G.H., Fan Y.R., Xu J.L., (2015). Hydrologic Risk Analysis for Nonstationary
792 Streamflow Records under Uncertainty. *Journal of Environmental Informatics*, 26(1), 41-51.

793 Lindenschmidt K.E., and Rokaya P., (2019). A Stochastic Hydraulic Modelling Approach to
794 Determining the Probable Maximum Staging of Ice-Jam Floods. *Journal of Environmental*
795 *Informatics*, 34(1) 45-54

796 Merz B, Thielen AH (2005) Separating natural and epistemic uncertainty in flood frequency
797 analysis. *Journal of Hydrology* 309(1–4):114–132

798 Metropolis, N., Rosenbluth, A. W., Rosenbluth, M. N., Teller, A. H. and Teller, E., (1953).
799 Equation of state by fast computing machines. *Journal Chemical Physics* 21, 1087–1092

800 Nelsen R.B., (2006). *An Introduction to Copulas*. Springer: New York.

801 Plummer, M., Best, N., Cowles, K., Vines, K., Sarkar, D., Bates, D., and Almond, R.: Package
802 coda, URL <http://cran.r-project.org/web/packages/coda/coda.pdf>, accessed January 25, 2015,
803 2015.

1
2
3
4
5
6
7
8
9
10
11
12
13
14
15
16
17
18
19
20
21
22
23
24
25
26
27
28
29
30
31
32
33
34
35
36
37
38
39
40
41
42
43
44
45
46
47
48
49
50
51
52
53
54
55
56
57
58
59
60
61
62
63
64
65

804 Requena A., Mediero L., Garrote L., (2013). A bivariate return period based on copulas for
805 hydrologic dam design: Accounting for reservoir routing in risk estimation. *Hydrology and*
806 *Earth System Sciences* 17(8):3023-3038

807 Salvadori G., De Michele C., Durante F., (2011). On the return period and design in a multivariate
808 framework. *Hydrology and Earth System Sciences* 15: 3293–3305

809 Salvadori, G., F. Durante, and C. De Michele (2013), Multivariate return period calculation via
810 survival functions, *Water Resources Research*, 49, 2308–2311, doi:10.1002/wrcr.20204

811 Salvadori G., De Michele C., Kottegoda N.T., Rosso R., (2007). *Extremes in Nature: an Approach*
812 *using Copula*. Springer: Dordrencht; 292

813 Salvadori, G., F. Durante, C. De Michele, M. Bernardi, and L. Petrella (2016), A multivariate
814 copula-based framework for dealing with hazard scenarios and failure probabilities, *Water*
815 *Resources Research*, 52, 3701–3721, doi:10.1002/2015WR017225.

816 Sak H., Yang G., Li B., and Li W., (2017). A copula-based model for air pollution portfolio risk
817 and its efficient simulation. *Stochastic Environmental Research and Risk Assessment*, 31(10),
818 2607-2616.

819 Sarhadi, A., D. H. Burn, M. C. Ausín, and M. P. Wiper (2016), Time-varying nonstationary
820 multivariate risk analysis using a dynamic Bayesian copula, *Water Resources Research*, 52,
821 2327–2349, doi:10.1002/2015WR01852

822 Serinaldi, F., 2013. An uncertain journey around the tails of multivariate hydrological distributions.
823 *Water Resources Research* 49, 6527–6547, doi:10.1002/wrcr.2053.

824 Serinaldi, F. (2015), Dismissing return periods!, *Stochastic Environmental Research and Risk*
825 *Assessment*, 29(4), 1179–1189, doi:10.1007/s00477-014-0916-1.

826 Shi W., Xia J., (2017). Combined risk assessment of nonstationary monthly water quality based on
827 Markov chain and time-varying copula. *Water Science and Technology*, 75(3-4), 693-704.

828 Song S., Singh V.P., (2010). Meta-elliptical copulas for drought frequency analysis of periodic
829 hydrologic data. *Stochastic Environmental Research and Risk Assessment*, 24(3), 425-444.

830 Spiegelhalter D., Gest N.G., Carlin B.P., Van Der Linde, A., (2002). Bayesian measures of model
831 complexity and fit. *Journal of the Royal Statistical Society, Series B*, 64(4), 583-639.

832 Sraj M., Bezak N., Brilly M. (2014). Bivariate flood frequency analysis using the copula function:
833 a case study of the Litija station on the Sava River. *Hydrological Processes*, 29(2), 225-238,
834 DOI: 10.1002/hyp.10145

835 Sun C.X., Huang G.H., Fan Y.R., Zhou X., Lu C., Wang X.Q. (2019). Drought Occurring with Hot
836 Extremes: Changes Under Future Climate Change on Loess Plateau, China. *Earth's Future*, 7,
837 587–604

838 The European Parliament and The Council (2007), Directive 2007/60/EC: On the assessment and
839 management of flood risks, Official Journal of the European Union, 116 pp

1
2
3
4
5
6
7
8
9
10
11
12
13
14
15
16
17
18
19
20
21
22
23
24
25
26
27
28
29
30
31
32
33
34
35
36
37
38
39
40
41
42
43
44
45
46
47
48
49
50
51
52
53
54
55
56
57
58
59
60
61
62
63
64
65

840 Vandenberghe S, Verhoest NEC, De Baets B. (2010). Fitting bivariate copulas to the dependence
841 structure between storm characteristics: a detailed analysis based on 105 year 10 min rainfall.
842 *Water Resources Research*, 46. DOI: 10.1029/2009wr007857.

843 Viglione, A, R. Merz, J.L. Salinas, G. Blschl (2013). Flood frequency hydrology: 3. A Bayesian
844 analysis, *Water Resources Research*, 49, 675-692.

845 Wang S., Huang G.H., Huang W., Fan Y.R., Li Z., (2015). A fractional factorial probabilistic
846 collocation method for uncertainty propagation of hydrologic model parameters in a reduced
847 dimensional space. *Journal of Hydrology*, 529, 1129-1146.

848 Wu H., Chen B., Snelgrove K., Lye L.M., (2019). Quantification of Uncertainty Propagation
849 Effects during Statistical Downscaling of Precipitation and Temperature to Hydrological
850 Modeling. *Journal of Environmental Informatics*, 34(2), 139-148.

851 Xu Y., Huang G.H., Fan Y.R., (2016). Multivariate flood risk analysis for Wei River. *Stochastic
852 Environmental Research and Risk Assessment*, 31 (1), 225-242 doi:
853 10.1007/s00477-015-1196-0

854 Yue S., (2000). The bivariate lognormal distribution to model a multivariate flood episode.
855 *Hydrological Processes*, 14(14), 2575-2588.

856 Yue S., (2001). A bivariate gamma distribution for use in multivariate flood frequency analysis.
857 *Hydrological Processes*, 15(6), 1033-1045

858 Zhang J.L., Li Y.P., Huang G.H., Chen X., Bao A.M., (2016). Assessment of parameter uncertainty
859 in hydrological model using a Markov-Chain-Monte-Carlo-based multilevel-factorial-analysis
860 method, *Journal of Hydrology*, 538, 471-486.

861 Zhang L., Singh V.P., (2006). Bivariate flood frequency analysis using the copula method. *Journal
862 of Hydrologic Engineering*, 11, 150-164.

863 Zhang L, Singh VP (2007) Bivariate rainfall frequency distributions using Archimedean copulas.
864 *Journal of Hydrology* 332(1–2):93–109

865 Zhang Q., Xiao M.Z., Singh V.P., (2015). Uncertainty evaluation of copula analysis of
866 hydrological droughts in the East River basin, China. *Global and Planetary Change*, 129, 1-9.

867
868

869 **Captions of Tables**

870 **Table 1.** Flood characteristics for different stations

871 **Table 2.** Model selection results by DIC and parameter estimation by MCMC

872 **Table 3.** ANOVA table for failure probability in OR

873

874 **Captions of Figures**

875 **Figure 1.** Framework of the proposed factorial Bayesian copula approach

876 **Figure 2.** The location of the studied watersheds. Wei River is the largest tributary of
877 Yellow river, with a drainage area of 135,000 km². The historical flood data from
878 Xianyang and Zhangjiashan stations on the Wei River are analyzed through the
879 proposed FBC approach. The Xiangxi River is located in the Three Gorges Reservoir
880 area with a drainage area of 3,200 km². The historical data from Xingshan station is
881 used in this study.

882 **Figure 3.** Posterior distributions of parameters in the copula models for different
883 gauge stations

884 **Figure 4.** Uncertainty in flood peak and volume inference at the three gauge stations:
885 both inferred flood peak and volume contain extensive uncertainties due to
886 randomness in model parameters; such uncertainties increase significantly the
887 increase in predefined return period

888 **Figure 5.** Uncertainty quantification of the joint return period in “OR”: the blue dash
889 lines indicate the predictive means and the red dash lines indicate the 5% and 95%
890 quantiles.

891 **Figure 6.** Uncertainty quantification for the failure probabilities in OR, AND and
892 Kendall at the Xingshan, Xianyang and Zhangjiashan stations: Considerable
893 uncertainties are observed in all failure probabilities and such uncertainties would
894 increase with the increase in service time

895 **Figure 7.** Main effects plot and full interactions plot matrix for parameters on the
896 failure probability in OR at the three gauge stations

897 **Figure 8.** Contributions of model parameters on uncertainty in predictive failure
898 probabilities of OR at the three gauge stations

899

1
2
3
4
5
6
7
8
9
10
11
12
13
14
15
16
17
18
19
20
21
22
23
24
25
26
27
28
29
30
31
32
33
34
35
36
37
38
39
40
41
42
43
44
45
46
47
48
49
50
51
52
53
54
55
56
57
58
59
60
61
62
63
64
65

Table 1. Flood characteristics for different stations

| Station name | period | | flood variable | |
|--------------|-----------|---------|--------------------------|----------------------------------|
| | | | Peak (m ³ /s) | Volume (m ³ /(s day)) |
| | | Minimum | 91 | 72 |
| Xingshan | 1961-2010 | Median | 451.5 | 713.3 |
| | | Maximum | 1050 | 2430 |
| | | Minimum | 139 | 317 |
| Xianyang | 1960-2006 | Median | 1350 | 2491 |
| | | Maximum | 12380 | 17802 |
| | | Minimum | 217 | 303.7 |
| Zhangjiashan | 1958-2012 | Median | 775 | 1365.3 |
| | | Maximum | 3730 | 7576.1 |

1
2
3
4
5
6
7
8
9
10
11
12
13
14
15
16
17
18
19
20
21
22
23
24
25
26
27
28
29
30
31
32
33
34
35
36
37
38
39
40
41
42
43
44
45
46
47
48
49
50
51
52
53
54
55
56
57
58
59
60
61
62
63
64
65

1
2
3
4
5
6
7
8
9
10
11
12
13
14
15
16
17
18
19
20
21
22
23
24
25
26
27
28
29
30
31
32
33
34
35
36
37
38
39
40
41
42
43
44
45
46
47
48
49

Table 2. Model selection results by DIC and parameter estimation by MCMC

| Stations | Attributes | Selected Distribution | Parameters | | | DIC | |
|--------------|------------|-----------------------|------------|--------------|--------------|---------------|---------|
| | | | α | β | θ | | |
| Xingshan | Peak | LN | Mean | 6.13 | 0.51 | - | 1403.77 |
| | | | 95% PI | [5.99, 6.27] | [0.43, 0.60] | - | |
| | Volume | LN | Mean | 6.67 | 0.62 | - | |
| | | | 95% PI | [6.49, 6.85] | [0.52, 0.72] | - | |
| | Copula | Gumbel | Mean | - | - | 2.34 | |
| | | | 95% PI | - | - | [1.86, 2.73] | |
| Zhangjiashan | Peak | LN | Mean | 6.63 | 0.65 | - | 1677.35 |
| | | | 95% PI | [6.48, 6.79] | [0.58, 0.76] | - | |
| | Volume | LN | Mean | 7.20 | 0.86 | - | |
| | | | 95% PI | [7.00, 7.41] | [0.75, 0.98] | - | |
| | Copula | Frank | Mean | - | - | 11.13 | |
| | | | 95% PI | - | - | [8.49, 13.15] | |
| Xianyang | Peak | LN | Mean | 7.17 | 0.86 | - | 1583.36 |
| | | | 95% PI | [6.93, 7.40] | [0.74, 0.99] | - | |
| | Volume | LN | Mean | 7.79 | 0.94 | - | |
| | | | 95% PI | [7.52, 8.06] | [0.84, 1.10] | - | |
| | Copula | Frank | Mean | - | - | 10.67 | |
| | | | 95% PI | - | - | [8.08, 13.61] | |

Note: 95%PI: 95% predictive interval

1
2
3
4
5
6
7
8
9
10
11
12
13
14
15
16
17
18
19
20
21
22
23
24
25
26
27
28
29
30
31
32
33
34
35
36
37
38
39
40
41
42
43
44
45
46
47
48
49

Table 3. ANOVA table for failure probability in OR

| Parameter | Xiangshan | | | | | Xianyang | | | | | Zhangjiashan | | | | |
|-----------|-----------|-----|---------|---------|----------|----------|-----|---------|---------|----------|--------------|-----|---------|---------|----------|
| | SS | DF | MS | F-Value | P-value | SS | DF | MS | F-Value | P-value | SS | DF | MS | F-Value | P-value |
| A | 9679.0 | 2 | 4839.5 | 927.7 | < 0.0001 | 11330.0 | 2 | 5665.0 | 2108.7 | < 0.0001 | 7916.5 | 2 | 3958.2 | 1579.8 | < 0.0001 |
| B | 46186.7 | 2 | 23093.3 | 4427.0 | < 0.0001 | 47547.6 | 2 | 23773.8 | 8849.4 | < 0.0001 | 55688.1 | 2 | 27844.1 | 11112.7 | < 0.0001 |
| C | 10355.3 | 2 | 5177.7 | 992.6 | < 0.0001 | 11306.2 | 2 | 5653.1 | 2104.3 | < 0.0001 | 8649.6 | 2 | 4324.8 | 1726.1 | < 0.0001 |
| D | 35232.7 | 2 | 17616.3 | 3377.1 | < 0.0001 | 49436.6 | 2 | 24718.3 | 9200.9 | < 0.0001 | 64601.5 | 2 | 32300.8 | 12891.4 | < 0.0001 |
| E | 78.6 | 2 | 39.3 | 7.5 | 0.0007 | 1.2 | 2 | 0.6 | 0.2 | 0.7988 | 1.2 | 2 | 0.6 | 0.2 | 0.7862 |
| AB | 5529.8 | 4 | 1382.5 | 265.0 | < 0.0001 | 3055.0 | 4 | 763.7 | 284.3 | < 0.0001 | 2381.7 | 4 | 595.4 | 237.6 | < 0.0001 |
| AC | 278.3 | 4 | 69.6 | 13.3 | < 0.0001 | 180.7 | 4 | 45.2 | 16.8 | < 0.0001 | 101.4 | 4 | 25.4 | 10.1 | < 0.0001 |
| AD | 1061.0 | 4 | 265.2 | 50.8 | < 0.0001 | 799.6 | 4 | 199.9 | 74.4 | < 0.0001 | 768.9 | 4 | 192.2 | 76.7 | < 0.0001 |
| AE | 1.4 | 4 | 0.4 | 0.1 | 0.9914 | 0.1 | 4 | 0.0 | 0.0 | 0.9999 | 0.1 | 4 | 0.0 | 0.0 | 0.9999 |
| BC | 1558.3 | 4 | 389.6 | 74.7 | < 0.0001 | 765.8 | 4 | 191.4 | 71.3 | < 0.0001 | 722.5 | 4 | 180.6 | 72.1 | < 0.0001 |
| BD | 6481.6 | 4 | 1620.4 | 310.6 | < 0.0001 | 3392.9 | 4 | 848.2 | 315.7 | < 0.0001 | 5489.1 | 4 | 1372.3 | 547.7 | < 0.0001 |
| BE | 19.1 | 4 | 4.8 | 0.9 | 0.4568 | 0.5 | 4 | 0.1 | 0.0 | 0.9964 | 0.5 | 4 | 0.1 | 0.1 | 0.9946 |
| CD | 4967.3 | 4 | 1241.8 | 238.1 | < 0.0001 | 3226.5 | 4 | 806.6 | 300.3 | < 0.0001 | 2589.4 | 4 | 647.3 | 258.4 | < 0.0001 |
| CE | 2.3 | 4 | 0.6 | 0.1 | 0.9780 | 0.1 | 4 | 0.0 | 0.0 | 0.9999 | 0.0 | 4 | 0.0 | 0.0 | 1.0000 |
| DE | 17.3 | 4 | 4.3 | 0.8 | 0.5088 | 0.5 | 4 | 0.1 | 0.0 | 0.9961 | 0.5 | 4 | 0.1 | 0.1 | 0.9945 |
| Error | 1001.6 | 192 | 5.2 | | | 515.8 | 192 | 2.7 | | | 481.1 | 192 | 2.5 | | |
| Total SS | 122450.3 | 242 | | | | 131559.0 | 242 | | | | 149392.2 | 242 | | | |

Note: SS, DF, MS represent sum of squares, degrees of freedom, mean square, respectively; A and B denote the two parameters in lognormal distribution (i.e. P_{par1} and P_{par2}) for flood peak; C and D denote the two parameters in lognormal distribution (i.e. V_{par1} and V_{par2}) for flood volume; E indicates the parameter in the copula (i.e. Cop_{par}). P-values greater than 0.05 are highlighted in this table.

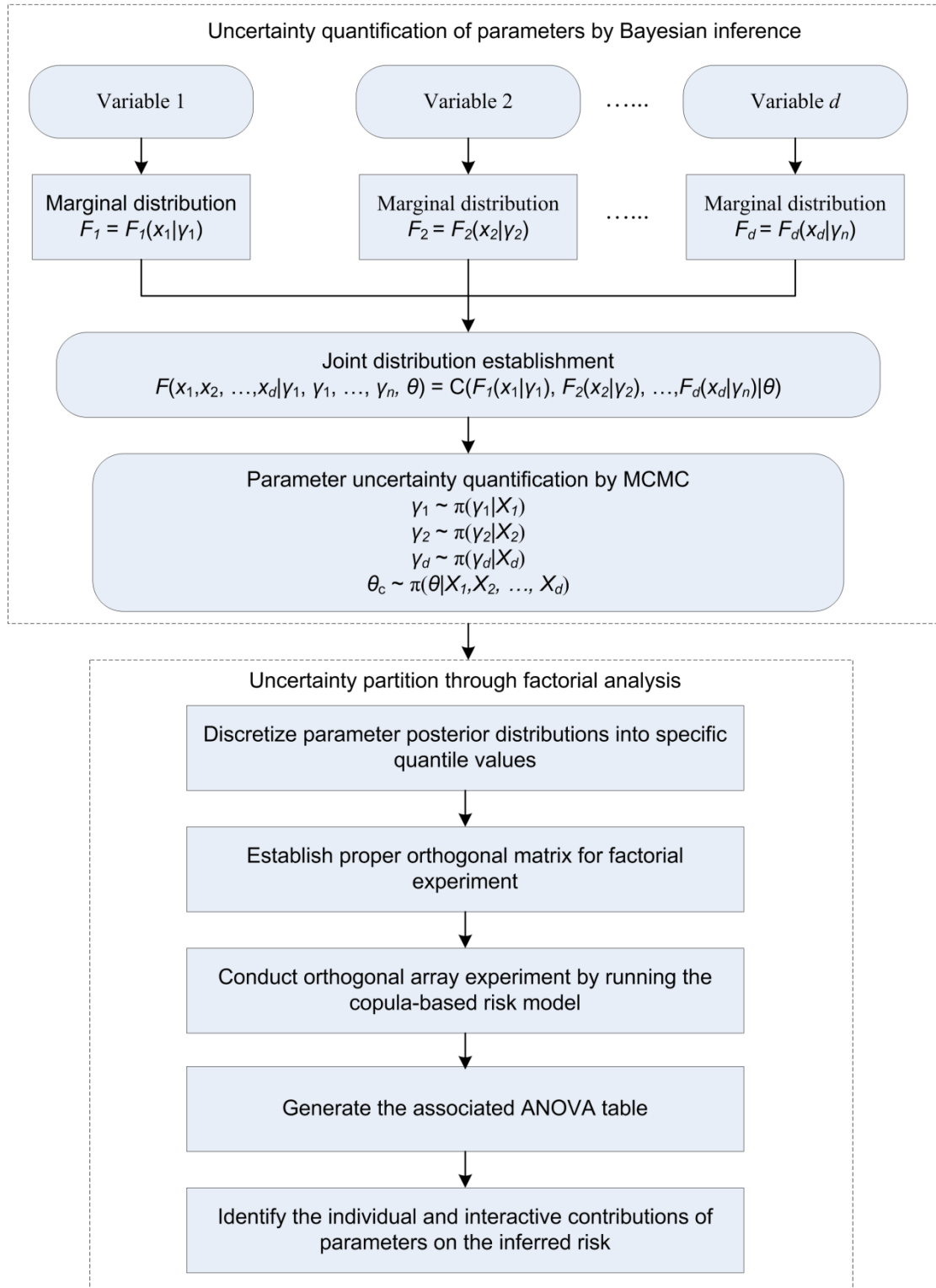


Figure 1. Framework of the proposed factorial Bayesian copula approach

1
2
3
4
5
6
7
8
9
10
11
12
13
14
15
16
17
18
19
20
21
22
23
24
25
26
27
28
29
30
31
32
33
34
35
36
37
38
39
40
41
42
43
44
45
46
47
48
49
50
51
52
53
54
55
56
57
58
59
60
61
62
63
64
65

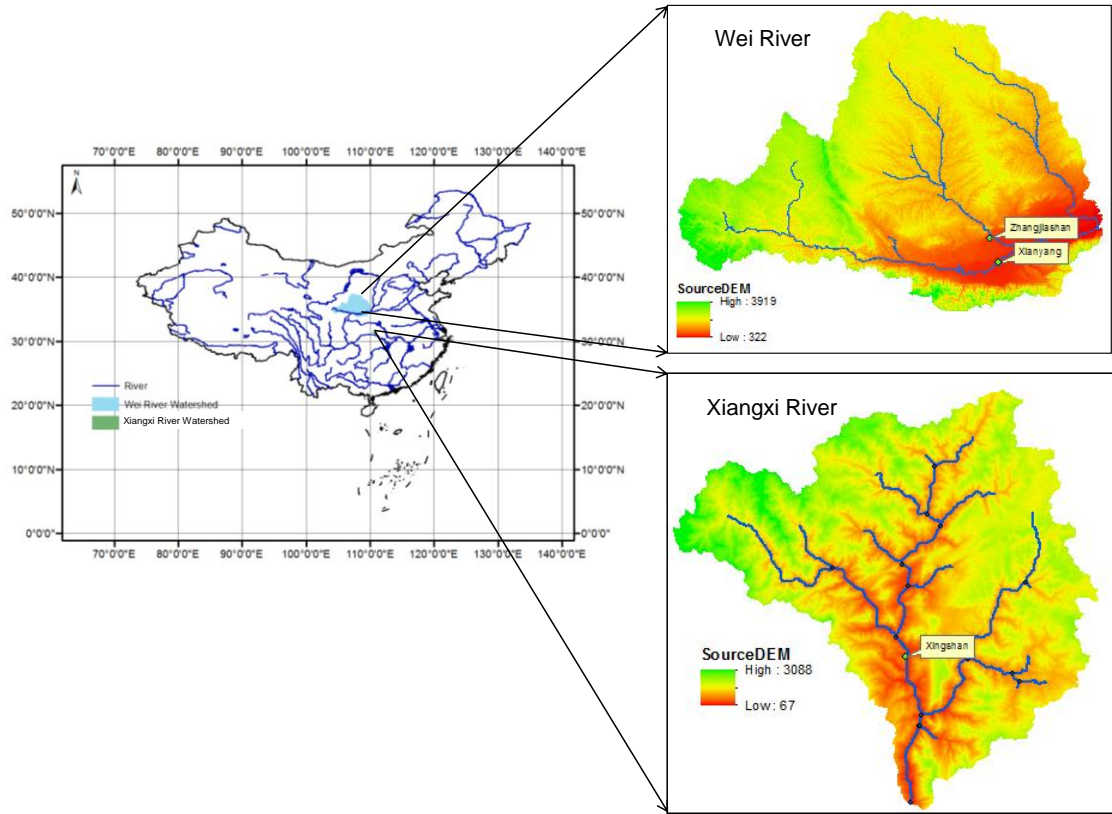


Figure 2. The location of the studied watersheds. Wei River is the largest tributary of Yellow river, with a drainage area of 135,000 km². The historical flood data from Xianyang and Zhangjiashan stations on the Wei River are analyzed through the proposed FBC approach. The Xiangxi River is located in the Three Gorges Reservoir area with a drainage area of 3,200 km². The historical data from Xingshan station is used in this study.

1
2
3
4
5
6
7
8
9
10
11
12
13
14
15
16
17
18
19
20
21
22
23
24
25
26
27
28
29
30
31
32
33
34
35
36
37
38
39
40
41
42
43
44
45
46
47
48
49

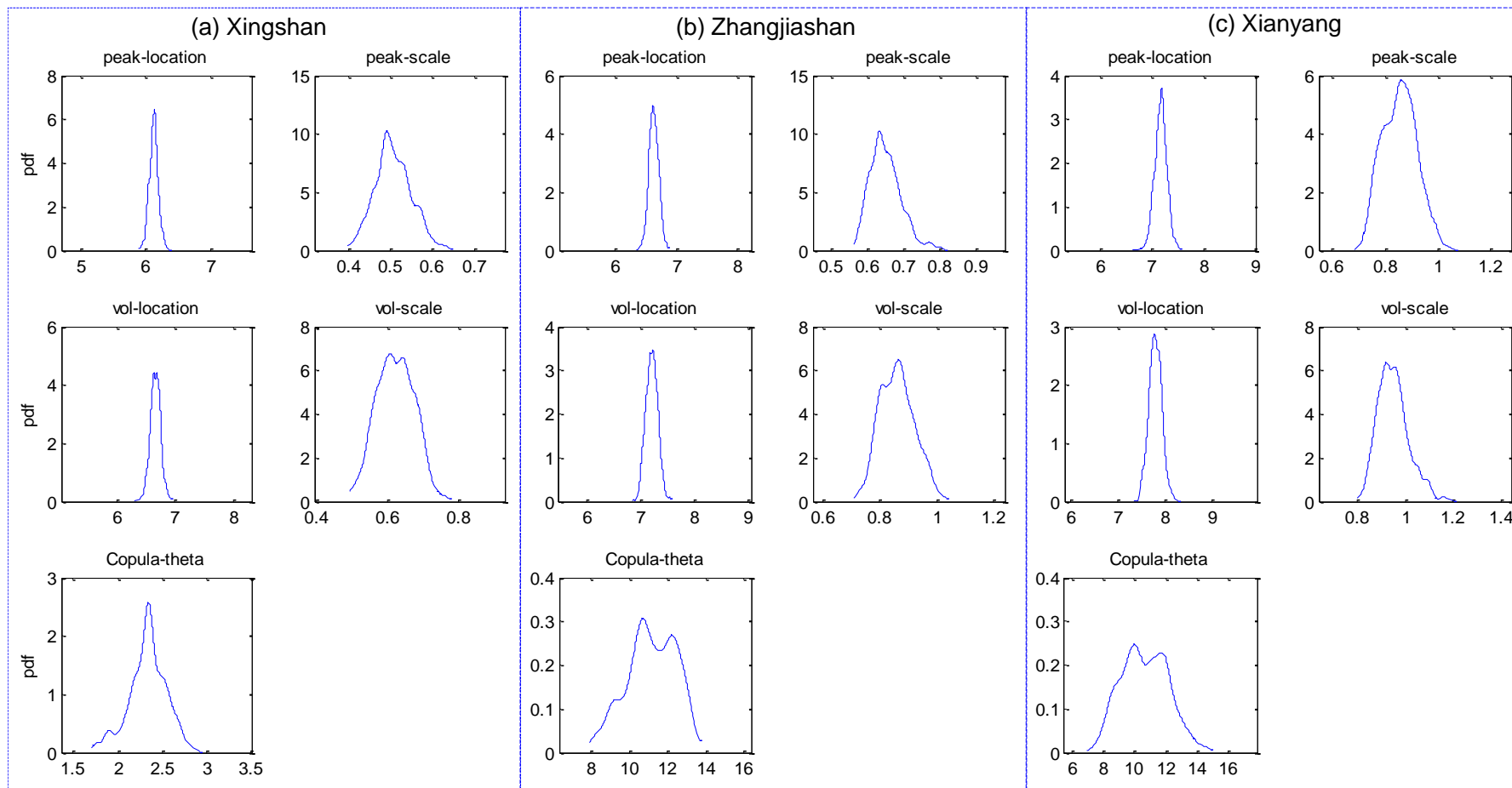


Figure 3. Posterior distributions of parameters in the copula models for different gauge stations

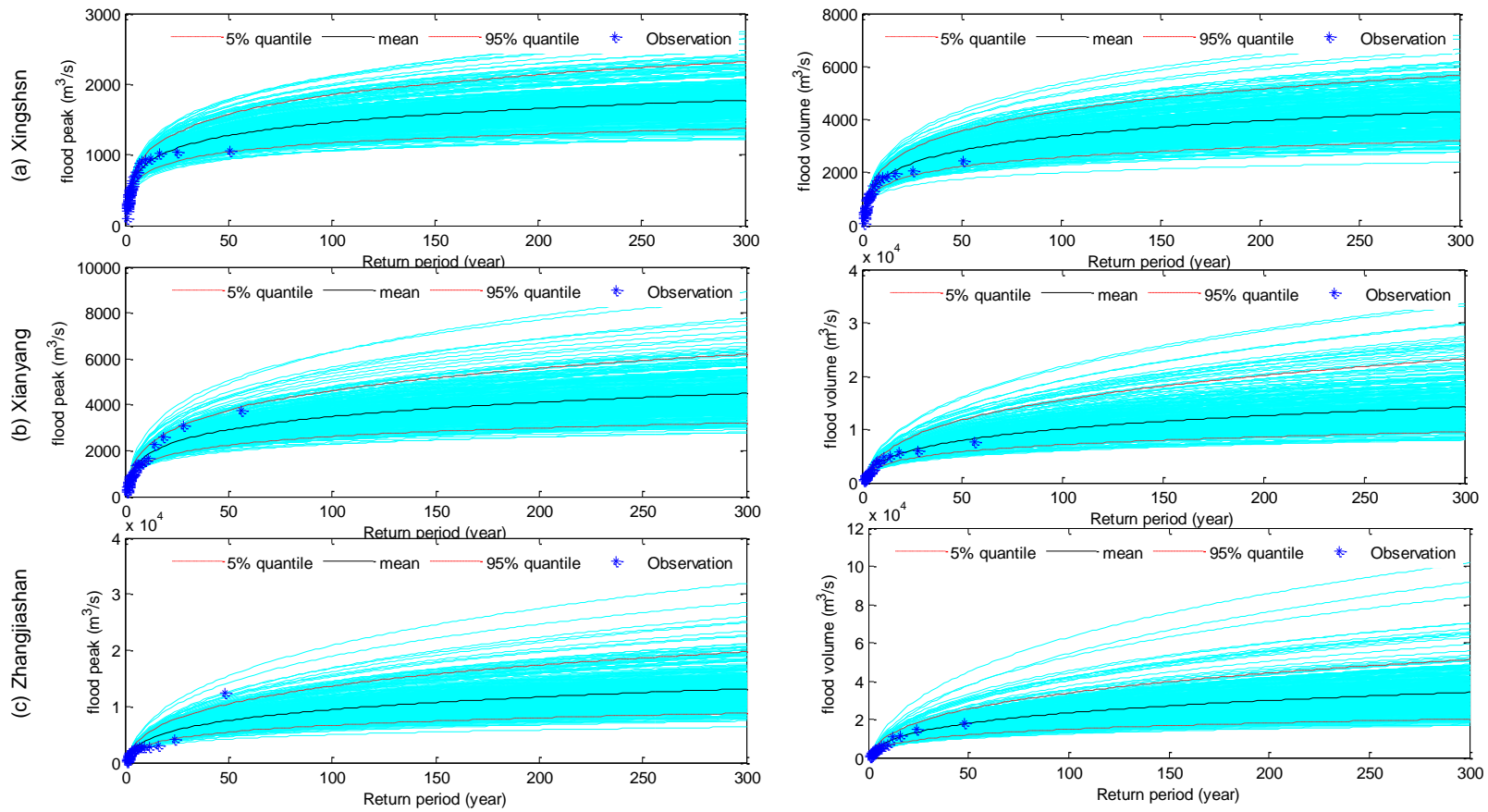


Figure 4. Uncertainty in flood peak and volume inference at the three gauge stations: both inferred flood peak and volume contain extensive uncertainties due to randomness in model parameters; such uncertainties increase significantly the increase in predefined return period

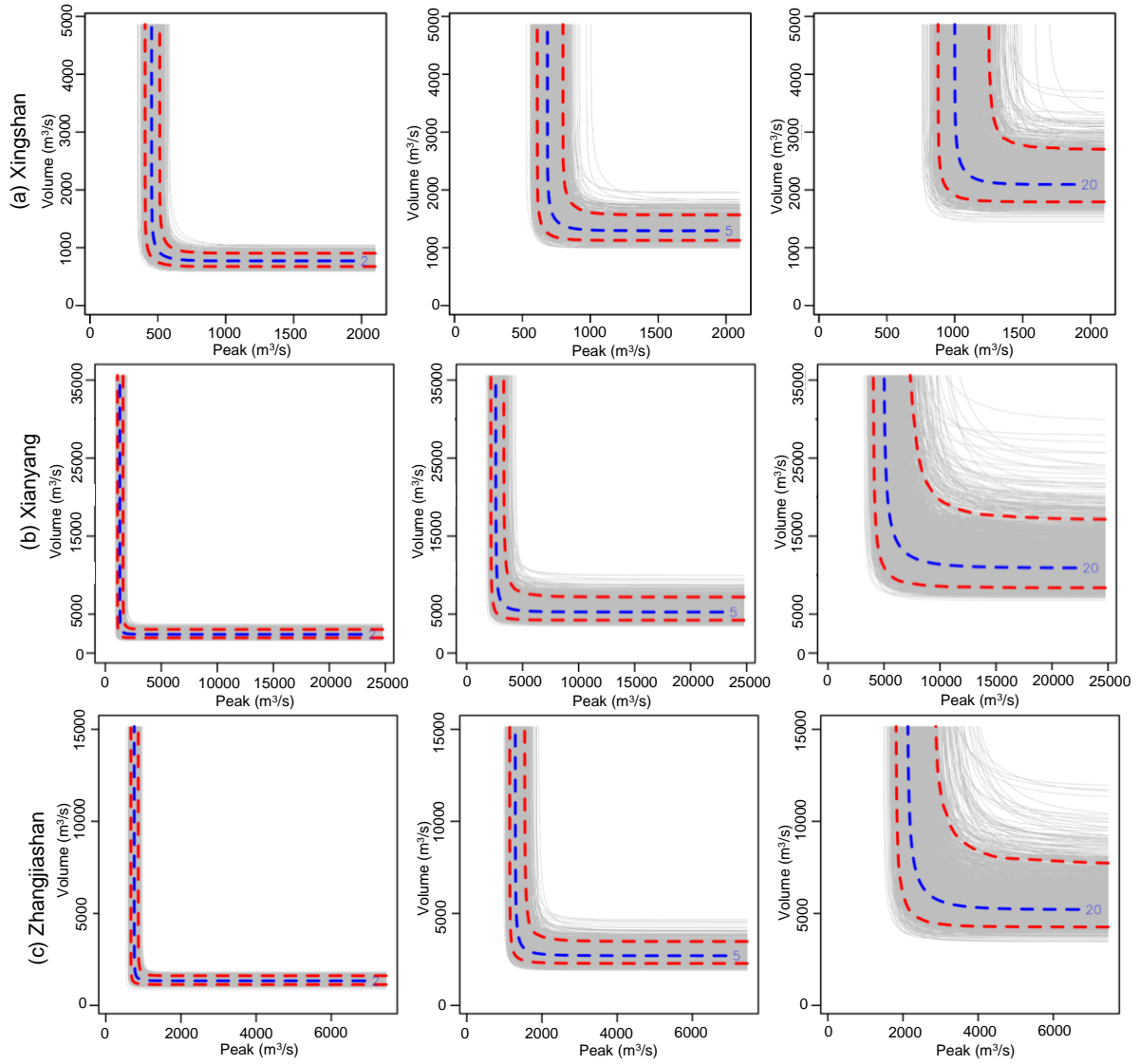


Figure 5. Uncertainty quantification of the joint return period in “OR”: the blue dash lines indicate the predictive means and the red dash lines indicate the 5% and 95% quantiles.

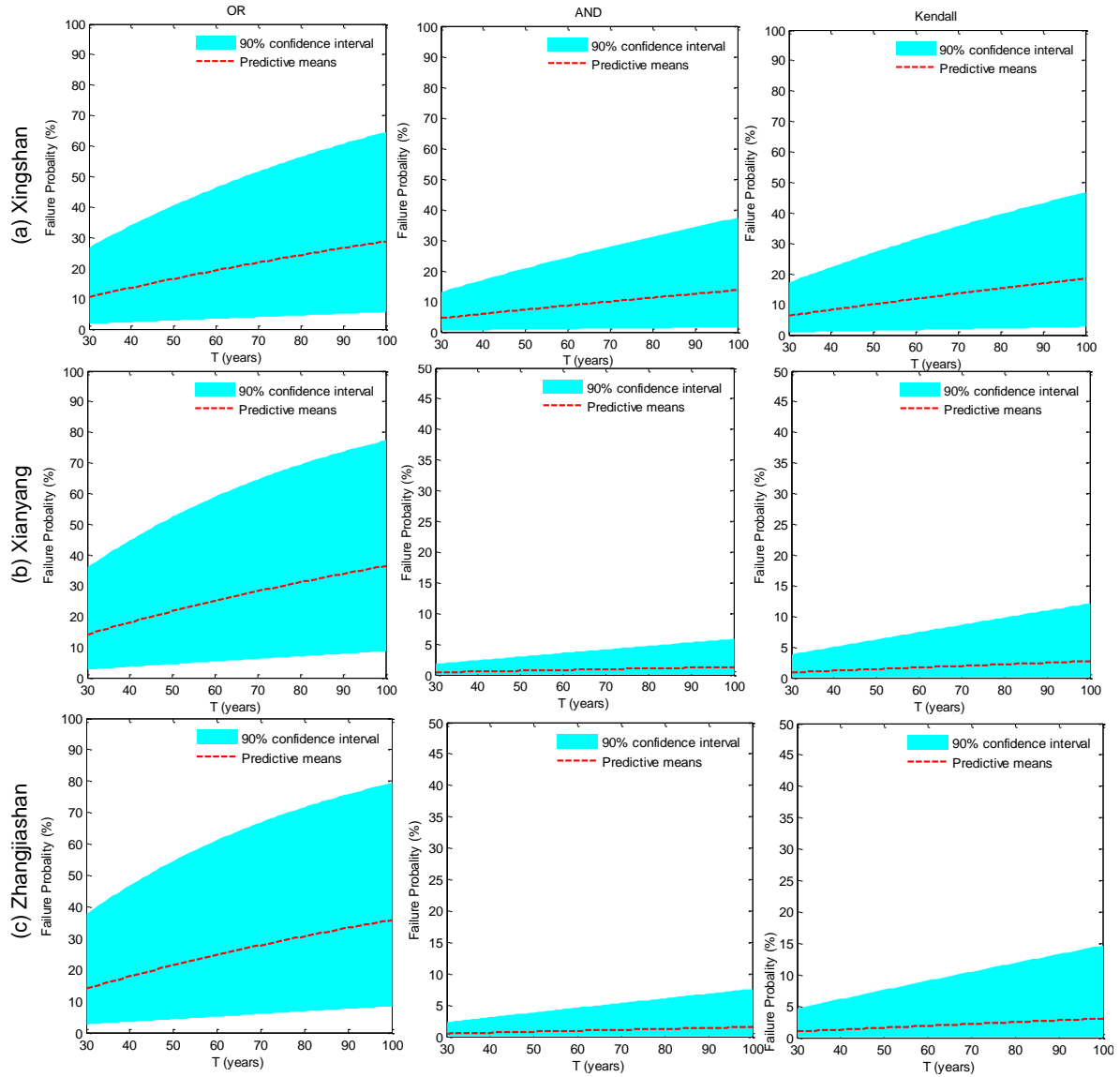


Figure 6. Uncertainty quantification for the failure probabilities in OR, AND and Kendall at the Xingshan, Xianyang and Zhangjiashan stations: Considerable uncertainties are observed in all failure probabilities and such uncertainties would increase with the increase in service time

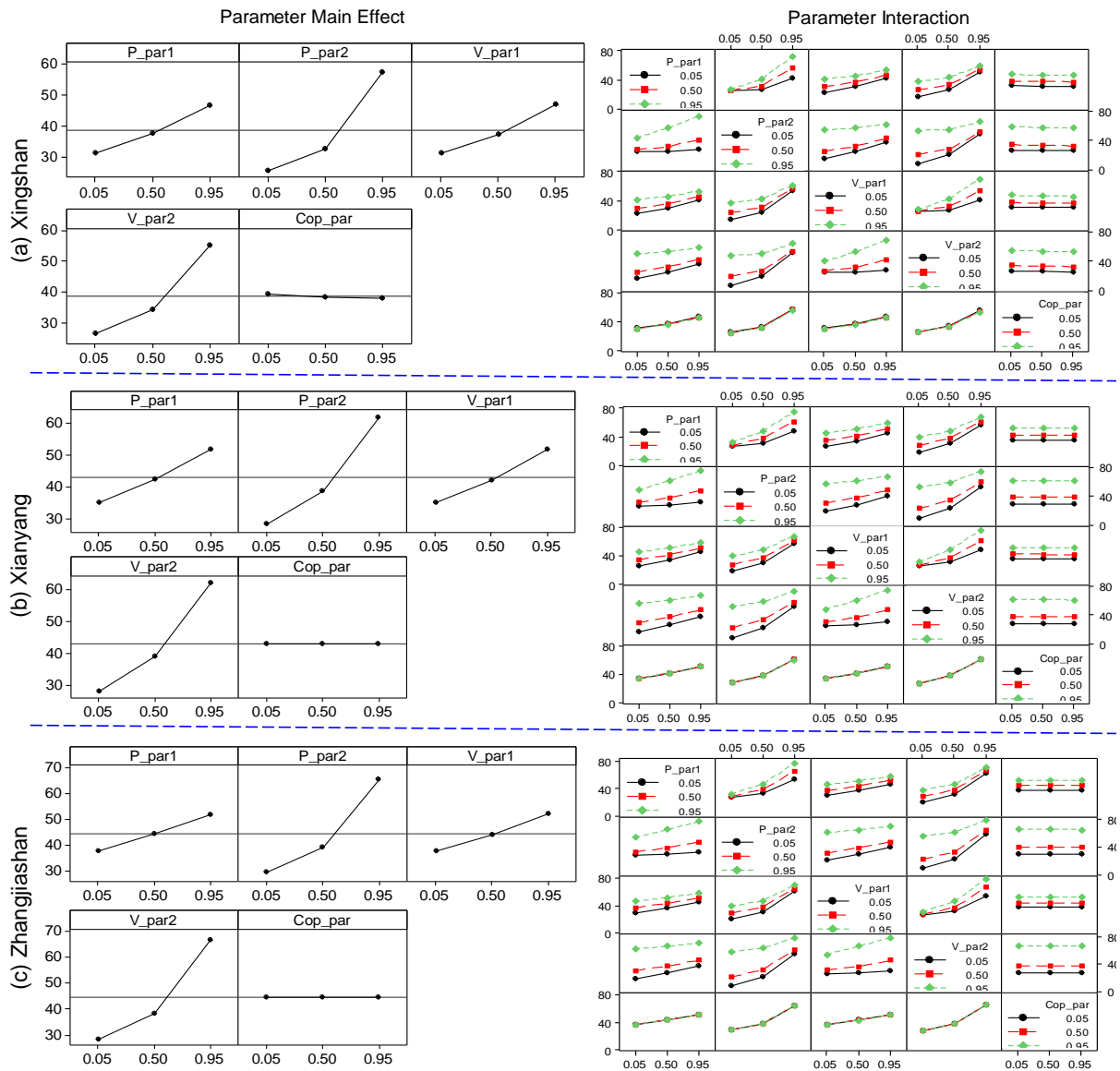


Figure 7. Main effects plot and full interactions plot matrix for parameters on the failure probability in OR at the three gauge stations

1
2
3
4
5
6
7
8
9
10
11
12
13
14
15
16
17
18
19
20
21
22
23
24
25
26
27
28
29
30
31
32
33
34
35
36
37
38
39
40
41
42
43
44
45
46
47
48
49

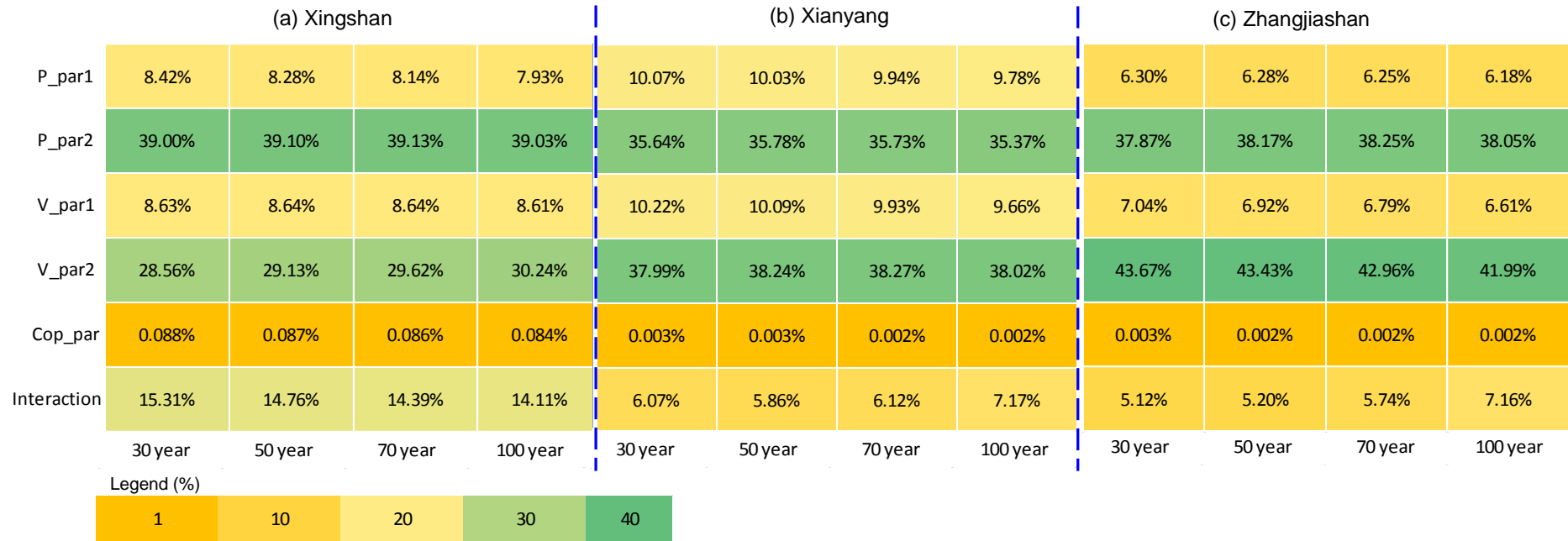


Figure 8. Contributions of model parameters on uncertainty in predictive failure probabilities of OR at the three gauge stations